

**Fig. 1.** CD134 interacts with HHV-6B gH/gL/gQ1/gQ2 and is expressed on HHV-6B permissive cells. (A) Purified HHV-6A- or HHV-6B gH/gL/gQ1/gQ2 complex was incubated with the lysates from Molt-3 cells whose cell surface was labeled with EZ-link sulfo-NHS-Lc-Biotin. The complex and its binding proteins were immunoblotted and detected with streptavidin, anti-CD46, or anti-CD134 antibody. (B) CD134 or CD46 expression on HHV-6B permissive and nonpermissive cells. HHV-6B permissive (Molt-3 and MT4) or nonpermissive (SupT1, JJhan, and HSB-2) cells were stained with anti-CD46 or CD134 antibody, followed by staining with secondary antibody for FACS analysis. Gray shading, isotype control. (C) Down-regulation of CD134 expression from the cell surface after HHV-6B infection. CD134 or CD46 expression on the surface of HHV-6B-infected Molt-3 cells was determined as described in B. Gray shading, isotype control; dark gray line, mock infection; light gray line, 2 h or 48 h postinfection (p.i.).

To confirm the identity of the corresponding band as CD134, immunoblotting was performed using the samples described above and an anti-CD134 antibody. The anti-CD134 antibody reacted with the eluate from the soluble HHV-6B gH/gL/gQ1/gQ2-bound resin but not with that from HHV-6A (Fig. 1A), indicating that CD134 associated specifically with the HHV-6B gH/gL/gQ1/gQ2 complex. On the other hand, an anti-CD46 antibody reacted with the eluate from the soluble HHV-6A gH/gL/gQ1/gQ2-bound resin but not with that from HHV-6B (Fig. 1A).

**Expression of CD134 in Several T-Cell Lines and Down-Regulation of CD134 on the Cell Surface by HHV-6B Infection.** HHV-6B permissive T-cell lines are distinct from those of HHV-6A. Therefore, next we assessed the level of CD134 protein expression in several T-cell lines by FACS analyses. CD134 was highly expressed in the HHV-6B permissive T-cell lines MT4 and Molt-3 but rarely in the HHV-6B nonpermissive T-cell lines HSB-2 and SupT1 (Fig. 1B). In contrast, CD46 was expressed abundantly in all of these cell lines (Fig. 1B).

In general the cellular receptor at the cell surface is down-regulated after viral infection. Therefore we examined the CD134 expression on the surface of HHV-6B-infected cells (Molt-3 cells). Fig. 1C shows that CD134 on the cell surface was down-regulated after HHV-6B infection, whereas the down-regulation of CD46 on the cell surface was rarely seen in the same condition.

**Inhibition of HHV-6B Infection by Soluble CD134 or Anti-CD134 Antibody.** We next examined whether a soluble CD134Fc could inhibit HHV-6B infection of cells. HHV-6 entry into cells was examined by observing the expression of the HHV-6 immediate-early protein, IE1. As shown in Fig. 2, soluble CD134Fc blocked

HHV-6B (HST strain) infection in a dose-dependent manner, whereas neither soluble Fc nor soluble CD46Fc did so. Notably, soluble CD134Fc did not block HHV-6A infection, although soluble CD46Fc did block it (Fig. 2, *Lower Left*), indicating that CD134 functions as an HHV-6B-specific receptor but not as a receptor for HHV-6A. We further examined whether CD134 also functions as the receptor for the other HHV-6B strains (Z29 and KYO), including clinical isolates. The results showed that sCD134Fc could block the other HHV-6B strains tested (Fig. 2, *Right*), confirming that CD134 functions as a specific cellular receptor for HHV-6B isolates.

Furthermore, we analyzed whether the anti-CD134 antibody blocks HHV-6B infection into target cells. When MT4 cells were infected with HHV-6B in the presence of anti-CD134 antibody, infection was blocked by the anti-CD134 antibody (Fig. 3). By contrast, control antibody did not affect HHV-6B infection into the cells (Fig. 3).

#### CD134-Expressing SupT1 Cells Become Susceptible for HHV-6B Infection.

Next, the CD134 gene was introduced into SupT1 cells, which are nonpermissive for HHV-6B infection, by a nonreplicative lentivirus, and HHV-6B was used to infect the CD134-overexpressing cells. The expression of CD134 on the SupT1 cells was confirmed by FACS (Fig. 4A). Notably, the CD134-expressing SupT1 cells were highly susceptible to HHV-6B entry (Fig. 4B), supporting the identification of CD134 as an HHV-6B receptor.

#### Specific Interaction of HHV-6B Glycoprotein Complex and CD134.

HHV-6A and -6B share 90% identity in their nucleic acid sequence. However, the amino acid sequences of gQ1 and gQ2 show low identity, with 78% and 69%, respectively, between HHV-6A and -6B compared with the sequences of gH and gL (11–13). Therefore, the gQ1 and gQ2 components of the gH/gL/gQ1/gQ2 complex may contribute to the virus specificity for different cellular receptors. To examine this possibility, several chimeric complexes were expressed in 293T cells. The cell-surface expression of each component in the complexes was confirmed. The binding of soluble CD134Fc to the surface of these cells was then measured by FACS. No CD134Fc binding was detected when AgH/AgL/AgQ1/AgQ2 (Fig. 5A and C), AgH/AgL/BgQ1/AgQ2 (Fig. 5B and C), or BgH/BgL/AgQ1/AgQ2 (Fig. 5A and C) was expressed in 293T cells, whereas CD134Fc

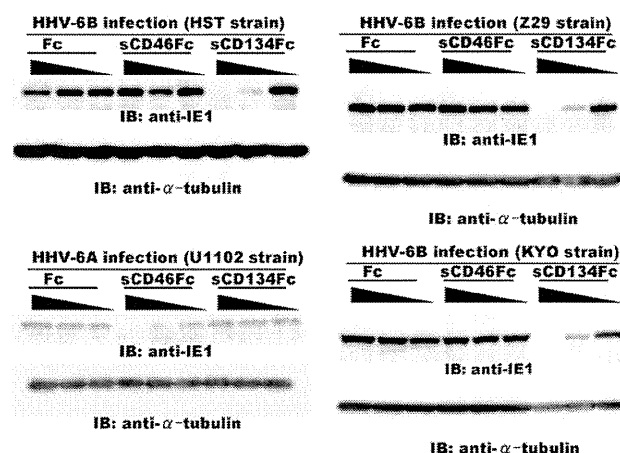


**Fig. 2.** CD134 is necessary for HHV-6B infection. HHV-6B (HST, KYO, or Z29 strain) or HHV-6A (U1102 strain) was incubated with the indicated amounts (diluted 10-fold from 2.5  $\mu$ g) of soluble CD134Fc, CD46Fc, or Fc, and then Molt-3 cells were infected with these viruses. The cell lysates were immunoblotted for HHV-6 immediate-early protein (BIE1 or AIE1) and  $\alpha$ -tubulin.

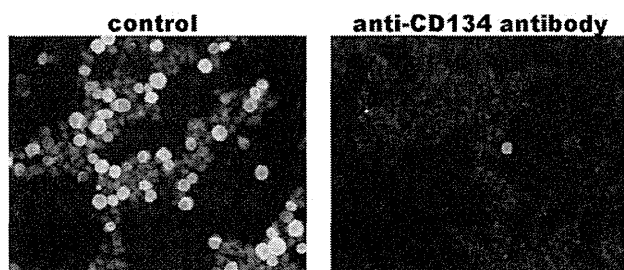


**Fig. 3.** Anti-CD134 antibody blocks HHV-6B infection. MT4 cells were infected with HHV-6B in the presence of anti-CD134 antibody (guinea pig serum) or control antibody (preimmune serum). The infection was examined by indirect immunofluorescence antibody assay using BIE1 antibody.

bound to 293T cells expressing BgH/BgL/BgQ1/BgQ2 (Fig. 5 *B* and *C*) or AgH/AgL/BgQ1/BgQ2 (Fig. 5 *B* and *C*), indicating that CD134 specifically bound to complexes containing HHV-6B gQ1 and gQ2. These data suggest that gQ1 and gQ2 of HHV-6B but not of HHV-6A in the complex are essential for binding to CD134.

### Discussion

Recently HHV-6B was classified as a separate species. Although its entry receptor has not been clear, here we found that CD134 is a cellular receptor specific for HHV-6B. Although HHV-6B and -6A share 90% identity in their nucleic acid sequence, they show distinct pathogenesis and cell tropism. The discovery of an HHV-6B-specific receptor supports the idea that the use of different receptors by HHV-6A and -6B is an important biological feature underlying their different characteristics and disease manifestations.

Previously we found that HHV-6A gH/gL/gQ1/gQ2 complex on the viral envelope is a viral ligand for CD46 (10, 16), which is a cellular receptor of HHV-6A (14). Here by using the soluble form of gH/gL/gQ1/gQ2 complex, we identified that the CD134 was a cellular receptor specific for HHV-6B. As predicted, the soluble form of HHV-6B gH/gL/gQ1/gQ2 complex bound to CD134, whereas that of HHV-6A did not. In addition, soluble CD134 could inhibit HHV-6B infection into target cells, whereas it could not inhibit HHV-6A infection, thus indicating that CD134 is a specific receptor for HHV-6B.

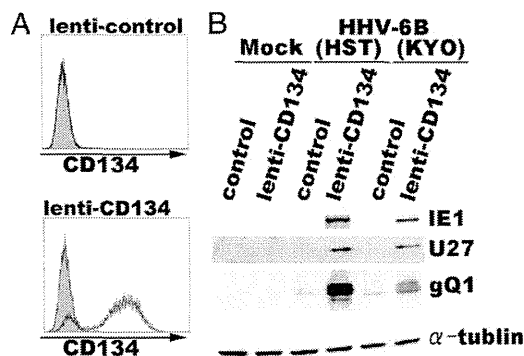


**Fig. 4.** SupT1 cells overexpressing CD134 become permissive for HHV-6B infection. (A) SupT1 cells were transduced with lentivirus or CD134-expressing lentivirus. CD134 expression on the SupT1 cells was confirmed by FACS analysis using an anti-CD134 antibody before HHV-6B infection. Gray shading, isotype control. (B) Four days later, the cells were infected with HHV-6B (HST or KYO strain), followed by immunoblotting with anti-HHV-6B IE1, -U27, -gQ1, and - $\alpha$ -tubulin antibodies.

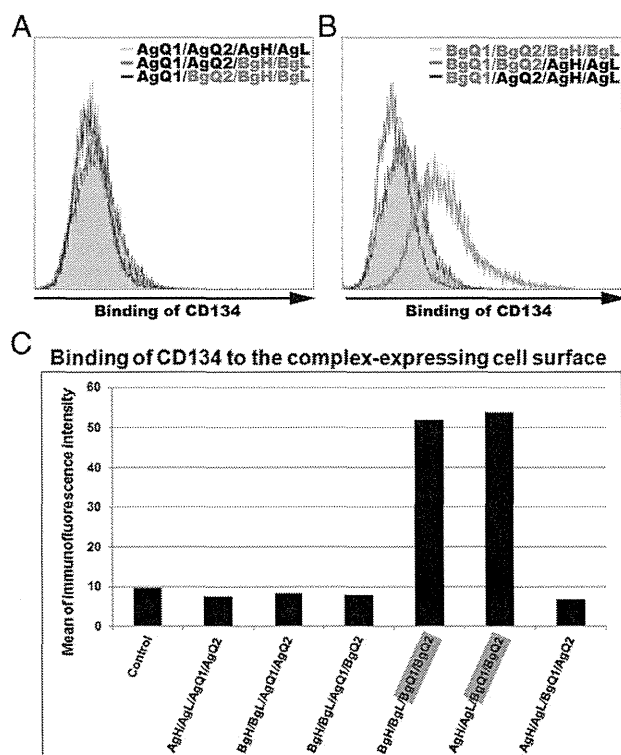


**Fig. 5.** HHV-6B-gQ1 and -gQ2 are the key molecules for HHV-6B's binding with CD134. (A and B) 293T cells were transfected with plasmids harboring individual molecules (indicated as different colors in histograms) or control plasmid (gray shading) and harvested 24 h later. The cells were incubated with soluble CD134Fc at 4 °C for 2 h and stained with Alexa Fluor 488 goat anti-human IgG antibody at 4 °C for 1 h for FACS analysis. (C) The intensity of immunofluorescence of the stained cells shown in A and B was quantified. A, HHV-6A; B, HHV-6B.

gQ1 and gQ2 in the complex are unique genes that are encoded specifically in HHV-6 and human herpesvirus-7 (HHV-7). In addition, HHV-6A and HHV-6B share low identity of them. Therefore we made several chimeric complexes of gQ1 and gQ2 and examined the interaction of chimeric complexes with CD134. Only the complex with HHV-6B gQ1 and gQ2 could bind to CD134, showing that gQ1 and gQ2 in the complex are crucial for the different receptor use between HHV-6B and HHV-6A.

CD134, which is also called OX40, is a member of the TNF receptor superfamily and is present on activated T lymphocytes, but it is rarely expressed on glial cells. HHV-6B is well known to have a cellular tropism for T lymphocytes, as shown in vivo during viremia from acute infection as well as in vitro (17, 18). Activated CD4<sup>+</sup> T lymphocytes are the preferred target of the fully permissive infection in vivo (18). Therefore, the present findings that strongly indicate CD134 is a functional HHV-6B entry receptor are consistent with the in vivo observations.

As described above, HHV-6B causes exanthem subitum in infants, and its reactivation causes encephalitis, especially in immunocompromised patients.

Because effective therapeutic agents for HHV-6B have not been developed, these findings may lead to new prophylactic and therapeutic approaches for HHV-6B-associated diseases, through the development of drugs that target CD134 and its regulators.

### Materials and Methods

**Plasmids.** An Fc fragment of human IgG1 with L266A and L267E mutations to reduce its binding affinity to cellular Fc receptors was used (19). The IL-2 signal sequence (amplified from pFuse-hlgG1-Fc2; Invivogen) was used in

place of the original signal sequence in each of the Fc fusion protein-expressing plasmids. In the CD46-expressing plasmid, the original signal sequence was used. To generate gHFcHis-expressing plasmids, the nucleic sequence for the ectodomain of gH (base pairs 46–2067) was amplified from the HHV-6A and -6B genomes by PCR, ligated with the Fc fragment containing a 6× histidine sequence at its 3' end, and cloned into the pCAGGS-MCS plasmid (20). Similarly, FcHis, CD46FcHis (base pairs 1–1029 of the CD46 sequence), and CD134FcHis (base pairs 85–642 of the CD134 sequence) were cloned into pCAGGS-MCS (provided by J. Miyazaki, Osaka University, Suita, Japan). We cloned the full-length CD134 sequence into CS-CA-MCS (provided by RIKEN: the Institute of Physical and Chemical Research; Japan) plasmid. The plasmids for expressing gQ1, gQ2, gH, and gL of HHV-6A and -6B were described previously (21, 22).

**Antibodies.** Mouse monoclonal antibodies to CD46 (J4, 48) and CD134 (Ber-ACT35) were purchased from Immunotech and BioLegend, respectively. The antibodies to IE1, U27, gH/gL, gH, gL, gQ1, and gQ2 of HHV-6A and HHV-6B were described previously (21–23). Anti-CD134 antibody was obtained by immunizing the purified CD134 protein to guinea pigs. Preimmune sera of guinea pigs were used as control antibody.

**Fc-Fusion Protein.** The plasmids for expressing Fc-fusion proteins were transfected into 293T cells using Lipofectamine 2000 (Invitrogen), according to the manufacturer's instructions. Two days after transfection, the soluble Fc-fusion proteins in the culture medium were purified by Ni-NTA (Qiagen) affinity chromatography.

**Identification of Proteins Associated with the BgH/BgL/BgQ1/BgQ2 Complex.** 293T cells were transfected with BgHFcHis-, BgL-, BgQ1-, and BgQ2-expressing plasmids or with AgHFcHis-, AgL-, AgQ1-, and AgQ2-expressing plasmids. The culture medium was harvested 48 h after transfection, incubated with Ni-NTA at 4 °C for 8 h, and then the Ni-NTA was spun down. Molt-3 cells (T-cell line) ( $1 \times 10^8$  cells per sample) were labeled with EZ-link sulfo-NHS-Lc-Biotin (Thermo Scientific) according to the manufacturer's protocol and lysed with TNE buffer [10 mM Tris-HCl (pH 7.8), 0.15 M NaCl, 1 mM EDTA, and 1% Nonidet P-40 (Nacalai Tesque)]. After centrifugation, the supernatant was incubated with the glycoprotein complex-bound Ni-NTA described above at 4 °C for 16 h. The proteins that bound to the Ni-NTA were eluted with 250 mM imidazole, and the buffer was changed to PBS using centrifugal filter devices (Millipore). Finally, the protein solution was incubated with protein G Sepharose at 4 °C for 8 h. The eluates were prepared for immunoblot analysis [using streptavidin-HRP (GE Healthcare) and silver staining (Invitrogen)]. The positive bands in the silver-stained gel (corresponding to the position of the positive band in the Western blot) were excised for in-gel digestion and LC-MS/MS analysis (24).

**Preparation of Virus Solution.** To prepare virus stocks, the viruses (HHV-6A and -6B strains) were propagated in umbilical cord blood mononuclear cells [CBMCs; provided by K. Adachi (Minoh Hospital, Minoh, Japan) and H. Yamada (Kobe University Graduate School of Medicine, Kobe, Japan) and purchased from the Cell Bank of the RIKEN Bioresource Center], which had been stimulated with 5 µg/mL phytohemagglutinin and 2 ng/mL IL-2 for 3 d. When more than 80% of the cells showed cytopathic effects, the cultures were frozen and thawed twice, then centrifuged at  $1,500 \times g$  for 5 min. The supernatants were collected and stored at –80 °C as cell-free virus stocks. We used CBMCs to titer the viruses by the 50% tissue culture infectious dose assay (25).

**Infection Inhibition Assay.** Cell-free HHV-6A or HHV-6B virus was incubated with soluble Fc, CD46Fc, or CD134Fc (diluted 10-fold from 2.5 µg) at 37 °C for 30 min, and then the virus was used to infect Molt-3 cells ( $5 \times 10^5$ ) at 37 °C for 1 h. The cells were cultured in 1 mL of medium for 24 h and then lysed with RIPA buffer [50 mM Tris (pH 7.4), 150 mM EDTA, 1% Triton X-100, 1% sodium deoxycholate, and 0.1% SDS] and used for immunoblotting analysis.

**Cell-Surface Expression Assay.** Cells were incubated with isotype control, anti-CD46, or anti-CD134 antibody at 4 °C for 1 h, followed by a secondary antibody. The cells were fixed with 4% (wt/vol) paraformaldehyde for 10 min before being analyzed on a FACSCalibur (BD).

**Cell-Surface Binding Assay.** Fc or soluble Fc-fusion proteins were incubated with a T-cell line (Molt-3 or SupT1) or with 293T cells transfected with glycoprotein-expressing plasmids (24 h after transfection) at 4 °C for 2 h, then the cells were washed with 3% (wt/vol) BSA/PBS and stained with an Alexa Fluor 488 goat anti-human IgG antibody (Invitrogen) at 4 °C for 1 h. The cells were washed with PBS, fixed with 4% (wt/vol) paraformaldehyde for 10 min, and then subjected to FACS analysis.

**Overexpression of CD134 in SupT1 Cells and Infection with HHV-6B.** CD134-expressing lentivirus and its control were constructed by transfecting 293T cells with CS-CA-MCS-CD134 (or its control, CS-CA-MCS) and packaging plasmids (pCAG-HIV-gag and pCMV-VSV-G-RSV-Rev provided by RIKEN). The culture media containing the viruses were harvested 3 d after transfection. SupT1 cells were transduced with the lentiviruses for 4 d and then infected with HHV-6B viruses. The cells were harvested and prepared for immunoblot analysis.

**ACKNOWLEDGMENTS.** We thank Y. Yamamoto (National Institute of Biomedical Innovation) and E. Moriishi (National Institute of Biomedical Innovation) for technical assistance, J. Miyazaki (Osaka University) for providing reagents, and K. Adachi (Minoh City Hospital) and H. Yamada (Kobe University) for the CBMCs. This work was supported by a Grant-in-Aid for Scientific Research (B) from the Japan Society for the Promotion of Science.

- Roizmann B, et al. (1992) The Herpesvirus Study Group of the International Committee on Taxonomy of Viruses (1992) The family Herpesviridae: An update. *Arch Virol* 123(3-4): 425–449.
- Salahuddin SZ, et al. (1986) Isolation of a new virus, HBLV, in patients with lymphoproliferative disorders. *Science* 234(4776):596–601.
- Aubin JT, et al. (1991) Several groups among human herpesvirus 6 strains can be distinguished by Southern blotting and polymerase chain reaction. *J Clin Microbiol* 29(2):367–372.
- Campadelli-Fiume G, Guerrini S, Liu X, Foa-Tomasi L (1993) Monoclonal antibodies to glycoprotein B differentiate human herpesvirus 6 into two clusters, variants A and B. *J Gen Virol* 74(Pt 10):2257–2262.
- Wyatt LS, Balachandran N, Frenkel N (1990) Variations in the replication and antigenic properties of human herpesvirus 6 strains. *J Infect Dis* 162(4):852–857.
- Yamanishi K, et al. (1988) Identification of human herpesvirus-6 as a causal agent for exanthem subitum. *Lancet* 1(8594):1065–1067.
- Okuno T, et al. (1989) Seroepidemiology of human herpesvirus 6 infection in normal children and adults. *J Clin Microbiol* 27(4):651–653.
- Pritchett JC, Nanau RM, Neuman MG (2012) The link between hypersensitivity syndrome reaction development and human herpes virus-6 reactivation. *Int J Hepatol* 2012:723062.
- Tohyama M, et al. (2007) Association of human herpesvirus 6 reactivation with the flaring and severity of drug-induced hypersensitivity syndrome. *Br J Dermatol* 157(5): 934–940.
- Mori Y (2009) Recent topics related to human herpesvirus 6 cell tropism. *Cell Microbiol* 11(7):1001–1006.
- Dominguez G, et al. (1999) Human herpesvirus 6B genome sequence: Coding content and comparison with human herpesvirus 6A. *J Virol* 73(10):8040–8052.
- Gompels UA, et al. (1995) The DNA sequence of human herpesvirus-6: Structure, coding content, and genome evolution. *Virology* 209(1):29–51.
- Isegawa Y, et al. (1999) Comparison of the complete DNA sequences of human herpesvirus 6 variants A and B. *J Virol* 73(10):8053–8063.
- Santoro F, et al. (1999) CD46 is a cellular receptor for human herpesvirus 6. *Cell* 99(7): 817–827.
- Akkapaboon P, Mori Y, Sadaoka T, Yonemoto S, Yamanishi K (2004) Intracellular processing of human herpesvirus 6 glycoproteins Q1 and Q2 into tetrameric complexes expressed on the viral envelope. *J Virol* 78(15):7969–7983.
- Mori Y, et al. (2004) Discovery of a second form of tripartite complex containing gH-gL of human herpesvirus 6 and observations on CD46. *J Virol* 78(9):4609–4616.
- Ablashi DV, et al. (1991) Genomic polymorphism, growth properties, and immunologic variations in human herpesvirus-6 isolates. *Virology* 184(2):545–552.
- Takahashi K, et al. (1989) Predominant CD4 T-lymphocyte tropism of human herpesvirus 6-related virus. *J Virol* 63(7):3161–3163.
- Shiratori I, Ogasawara K, Saito T, Lanier LL, Arase H (2004) Activation of natural killer cells and dendritic cells upon recognition of a novel CD99-like ligand by paired immunoglobulin-like type 2 receptor. *J Exp Med* 199(4):525–533.
- Niwa H, Yamamura K, Miyazaki J (1991) Efficient selection for high-expression transfectants with a novel eukaryotic vector. *Gene* 108(2):193–199.
- Kawabata A, et al. (2011) Analysis of a neutralizing antibody for human herpesvirus 6B reveals a role for glycoprotein Q1 in viral entry. *J Virol* 85(24):12962–12971.
- Tang H, Hayashi M, Maeki T, Yamanishi K, Mori Y (2011) Human herpesvirus 6 glycoprotein complex formation is required for folding and trafficking of the gH/gL/gQ1/gQ2 complex and its cellular receptor binding. *J Virol* 85(21):11121–11130.
- Mori Y, et al. (2002) Human herpesvirus 6 variant A but not variant B induces fusion from without in a variety of human cells through a human herpesvirus 6 entry receptor, CD46. *J Virol* 76(13):6750–6761.
- Shevchenko A, Wilm M, Vorm O, Mann M (1996) Mass spectrometric sequencing of proteins silver-stained polyacrylamide gels. *Anal Chem* 68(5):850–858.
- Asada H, Yalcin S, Balachandra K, Higashi K, Yamanishi K (1989) Establishment of titration system for human herpesvirus 6 and evaluation of neutralizing antibody response to the virus. *J Clin Microbiol* 27(10):2204–2207.

# Supporting Information

Tang et al. 10.1073/pnas.1305187110

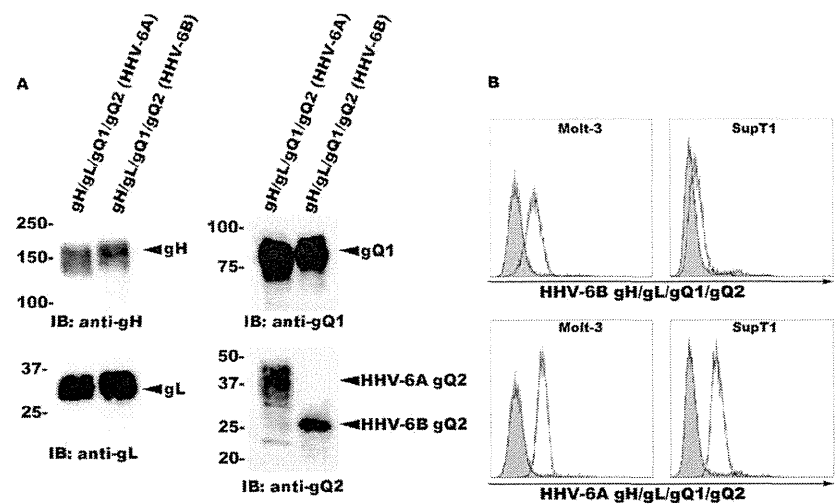


**Fig. S1.** Specific binding of soluble HHV-6B gH/gL/gQ1/gQ2 complex to virus permissive cells. (A) Secretion of the AgHFc/AgL/AgQ1/AgQ2 or BgHFc/BgL/BgQ1/BgQ2 complex. 293T cells were cotransfected with several plasmids harboring individual molecules. The culture medium was harvested 2 d after transfection, and the recombinant proteins were purified by Ni-NTA affinity chromatography and subjected to immunoblot analysis using antibodies for each component of the complex. (B) The HHV-6B ligand binds to Molt-3 (HHV-6B permissive) but not SupT1 (HHV-6B nonpermissive) cells. Molt-3 (HHV-6B permissive) or SupT1 (HHV-6B nonpermissive) cells were incubated with soluble HHV-6A- or HHV-6B gHFc/gL/gQ1/gQ2 complex at 4 °C for 2 h, stained with Alexa Fluor 488 goat anti-human IgG antibody at 4 °C for 1 h, and subjected to FACS analysis. Gray shading, incubated with Fc as control.

# CD34<sup>+</sup>/CD38<sup>−</sup> acute myelogenous leukemia cells aberrantly express CD82 which regulates adhesion and survival of leukemia stem cells

Chie Nishioka<sup>1,2</sup>, Takayuki Ikezoe<sup>3</sup>, Mutsuo Furihata<sup>4</sup>, Jing Yang<sup>3</sup>, Satoshi Serada<sup>5</sup>, Tetsuji Naka<sup>5</sup>, Atsuya Nobumoto<sup>6</sup>, Sayo Kataoka<sup>7</sup>, Masayuki Tsuda<sup>6</sup>, Keiko Udaka<sup>1</sup> and Akihito Yokoyama<sup>3</sup>

<sup>1</sup>Department of Immunology, Kochi Medical School, Kochi University, Nankoku, Kochi, Japan

<sup>2</sup>Japanese Society for the Promotion of Science (JSPS), Chiyoda-ku, Tokyo, Japan

<sup>3</sup>Hematology and Respiratory Medicine, Kochi Medical School, Kochi University, Nankoku, Kochi, Japan

<sup>4</sup>Tumor Pathology, Kochi Medical School, Kochi University, Nankoku, Kochi, Japan

<sup>5</sup>Laboratory for immune Signal, National Institute of Biomedical Innovation, Ibaraki, Osaka

<sup>6</sup>The Facility for Animal Research, Kochi Medical School, Kochi University, Nankoku, Kochi, Japan

<sup>7</sup>Medical Research Center, Kochi Medical School, Kochi University, Nankoku, Kochi, Japan

To identify molecular targets in leukemia stem cells (LSCs), this study compared the protein expression profile of freshly isolated CD34<sup>+</sup>/CD38<sup>−</sup> cells with that of CD34<sup>+</sup>/CD38<sup>+</sup> counterparts from individuals with acute myelogenous leukemia ( $n = 2$ , AML) using isobaric tags for relative and absolute quantitation (iTRAQ). A total of 98 proteins were overexpressed, while six proteins were underexpressed in CD34<sup>+</sup>/CD38<sup>−</sup> AML cells compared with their CD34<sup>+</sup>/CD38<sup>+</sup> counterparts. Proteins overexpressed in CD34<sup>+</sup>/CD38<sup>−</sup> AML cells included a number of proteins involved in DNA repair, cell cycle arrest, gland differentiation, antiapoptosis, adhesion, and drug resistance. Aberrant expression of CD82, a family of adhesion molecules, in CD34<sup>+</sup>/CD38<sup>−</sup> AML cells was noted in additional clinical samples ( $n = 12$ ) by flow cytometry. Importantly, down-regulation of CD82 in CD34<sup>+</sup>/CD38<sup>−</sup> AML cells by a short hairpin RNA (shRNA) inhibited adhesion to fibronectin *via* up-regulation of matrix metalloproteinases 9 (MMP9) and colony forming ability of these cells as assessed by transwell assay, real-time RT-PCR, and colony forming assay, respectively. Moreover, we found that down-regulation of CD82 in CD34<sup>+</sup>/CD38<sup>−</sup> AML cells by an shRNA significantly impaired engraftment of these cells in severely immunocompromised mice. Taken together, aberrant expression of CD82 might play a role in adhesion of LSCs to bone marrow microenvironment and survival of LSCs. CD82 could be an attractive molecular target to eradicate LSCs.

**Key words:** AML, leukemia stem cells, bone marrow microenvironment, CD82, MMP9

Additional Supporting Information may be found in the online version of this article.

\*Takayuki Ikezoe contributed to the concept and design, interpreted and analyzed the data and wrote an article. Chie Nishioka performed all experiments and wrote an article. Mutsuo Furihata, Jing Yang, Satoshi Serada, and Tetsuji Naka, Sayo Kataoka and Atsuya Nobumoto performed the experiments. Akihito Yokoyama and Keiko Udaka provided important intellectual content

**Grant sponsors:** The Kochi University President's Discretionary Grant, Setsuro Fujii Memorial, The Osaka Foundation for Promotion of Fundamental Medical Research, Certificate of Kochi Shin-kin/Anshin-tomo-no-kai Prize and Japan Society for the Promotion of Science

**DOI:** 10.1002/ijc.27904

**History:** Received 15 Mar 2012; Accepted 25 Sep 2012; Online 11 Oct 2012

**Correspondence to:** Takayuki Ikezoe, Department of Hematology and Respiratory Medicine, Kochi University, Oko-cho, Nankoku, Kochi 783-8505, Japan, Tel.: 81-88-880-2345, Fax: 81-88-880-2348, E-mail: ikezoet@kochi-u.ac.jp

Acute myelogenous leukemia (AML) is characterized by a cellular hierarchy, and is initiated and maintained by a subset of self-renewing leukemia stem cells (LSCs).<sup>1</sup> To produce cure in individuals with AML, development of a novel treatment strategy targeting LSCs is urgently required. LSCs share some antigenic features with normal hematopoietic stem cells (HSCs). For example, both LSCs and HSCs express CD34 but not CD38. However, LSCs can be phenotypically distinguished from HSCs by several disparate markers, including CD117<sup>−</sup> and CD123<sup>+</sup>.<sup>1–3</sup> LSCs exist in a quiescent state and are capable of self-renewal and differentiation, and are able to perpetuate leukemic cell growth in long-term culture assays and in the murine nonobese diabetic/severe combined immunodeficiency (NOD/SCID) model system.<sup>1–4</sup> CD34<sup>+</sup>/CD38<sup>−</sup> AML cells were shown to fulfill the criteria for LSCs *in vivo*.<sup>5,6</sup> Although, recent studies employed more severely immunocompromised mice found that even CD34<sup>−</sup> or CD38<sup>+</sup> AML cells in some cases were able to reconstitute AML.<sup>7,8</sup>

The regulation of stem cell self-renewal and differentiation requires a specific microenvironment of surrounding cells known as the stem cell niche. The concept of the stem cell niche was first proposed for the human hematopoietic system in the 1970s.<sup>9</sup> The HSC niche in mouse bone marrow (BM) is

**What's new?**

Acute myelogenous leukemia (AML) is maintained by a subset of self-renewing leukemia stem cells (LSCs). Thus, to effectively treat AML, treatments targeting LSCs are needed. AML cells expressing CD34 but not CD38 (CD34<sup>+</sup>/CD38<sup>-</sup>) contain abundant LSCs and were found in this study to express a greater amount of CD82 than CD34<sup>+</sup>/CD38<sup>+</sup> AML cells. CD82 was further found to regulate the survival of CD34<sup>+</sup>/CD38<sup>-</sup> AML cells and their adhesion to the bone marrow microenvironment, suggesting that this glycoprotein could be an attractive target for LSC eradication.

composed of an endosteal lining of stromal cells, extracellular matrix proteins, and osteoblasts.<sup>10–12</sup> Specific adherens junction molecules such as N-cadherin mediate adhesion between HSCs and niche cells in the adult hematopoietic system.<sup>11</sup>

Recent work has shown that interaction between CXCR4 on leukemic cells and its ligand stromal cell-derived factor-1 (SDF-1) in the niche is necessary for proper homing and *in vivo* growth of leukemic cells.<sup>13</sup> Moreover, interaction between LSCs and the niche mediated by adhesion molecule CD44 is required for maintenance of LSCs behavior.<sup>14</sup> CD44 mediates adhesive cell-cell and cell-extracellular matrix interactions by binding its main ligand, hyaluronan, a glycosaminoglycan that is highly concentrated in the endosteal region.<sup>14,15</sup> All together, adhesion molecules play an important role in maintaining the characteristics of LSCs.

CD82/KAI-1, a member of the tetraspanin superfamily, was originally identified as an accessory molecule in T-cell activation.<sup>16</sup> The most well-characterized function of CD82 in nonimmune cells is integrin-mediated cell adhesion to extracellular matrix.<sup>17</sup> Forced expression of CD82 up-regulated tissue inhibitors of metalloproteinase 1 (TIMP1) and inactivated matrix metalloproteinases 9 (MMP9) in the H1299 human lung carcinoma cells, resulting in suppression of tumor invasion and metastasis.<sup>18</sup> Cell adhesion to collagen I, which is one of the major proteins in the bone marrow (BM) niche, is mostly mediated by three integrin receptors  $\alpha 1 \beta 1$ ,  $\alpha 2 \beta 1$ , and  $\alpha 11 \beta 1$  expressed on cell surface of mesenchymal stem cells.<sup>19</sup> Integrin may associate with CD82 in CD34<sup>+</sup>/CD38<sup>-</sup> AML cells to promote adhesion to the endosteal niche. However, the roles of CD82 in hematopoietic cells remain to be elucidated.

In this study, we analyzed the protein expression profile of freshly isolated CD34<sup>+</sup>/CD38<sup>-</sup> AML cells from individuals with AML and compared it with the expression profile of their CD34<sup>+</sup>/CD38<sup>+</sup> counterparts using isobaric tags for relative and absolute quantitation (iTRAQ) and found the aberrant expression of CD82 in CD34<sup>+</sup>/CD38<sup>-</sup> AML cells. This study also explored the function of CD82 in CD34<sup>+</sup>/CD38<sup>-</sup> AML cells *in vitro* as well as *in vivo* by utilizing NOD.Cg-*Rag1<sup>tm1Mom</sup> Il2rg<sup>tm1Wjl</sup>/SzJ* mice.

**Material and Methods****Sample collection and isolation of CD34<sup>+</sup>/CD38<sup>-</sup> AML cells and their CD34<sup>+</sup>/CD38<sup>+</sup> counterparts**

Leukemia cells were freshly isolated from AML patients (*n* = 18) with World Health Organization (WHO) classifica-

tion system subtype minimally differentiated AML (case 6), AML without maturation (cases 1 and 10), AML with maturation (cases 2, 7, and 12), acute myelomonocytic leukemia (cases 4, 14, and 15), AML with myelodysplasia changes (cases 3, 5, 8, 9, 16, 17, and 18), and therapy-related AML (cases 11 and 13) after obtaining informed consent with Kochi University Institutional Review Board approval (Supporting Information Table S1). The informed consent was obtained in accordance with the Declaration of Helsinki. CD34<sup>+</sup>/CD38<sup>-</sup> AML cells and CD34<sup>+</sup>/CD38<sup>+</sup> counterparts were purified by magnetic cell sorting utilizing a CD34 MultiSort kit and a CD38 MicroBead kit (Miltenyi Biotec GmbH, Germany), as previously described (Supporting Information Fig. S1a).<sup>20</sup>

**Cells**

Chronic eosinophilic leukemia (CEL) EOL-1 cells were obtained from RIKEN BRC Cell Bank (Tsukuba, Japan). Imatinib-resistant EOL-1R cell line was established by culturing with increasing concentrations of imatinib (from 1 to 100 nM) for 6 months.<sup>21</sup> Most of EOL-1R cells expressed CD34 (92 ± 9%) on their cell surface. On the other hand, CD34 was rarely detectable on cell surface of parental EOL-1 cells (0.1 ± 0.1%) (figure not shown).

**Isolation and culture of primary mesenchymal stromal cells (MSCs)**

MSCs were isolated from a BM of healthy donors. BM cells were subjected to centrifugation over a Ficoll-Hypaque gradient to separate mononuclear cells. These cells were resuspended in  $\alpha$ -minimal essential medium (Gibco BRL, Rockville, MD) containing 20% fetal bovine serum (FBS) and plated at an initial density of 10<sup>6</sup> cells.<sup>22</sup>

**Protein extraction**

Proteins were extracted using the complete mammalian proteome kit (539779, Calbiochem, Darmstadt, Germany), according to the manufacturer's instructions.

**iTRAQ labeling of peptides**

Each protein sample (100  $\mu$ g) was digested with trypsin and labeled with iTRAQ reagents (Applied Biosystems, Framingham, MA) according to the manufacturer's instructions. Briefly, the proteins extracted from CD34<sup>+</sup>/CD38<sup>-</sup> AML cells were labeled with iTRAQ reagents 114 (case 1) or 116 (case 2), and proteins extracted from CD34<sup>+</sup>/CD38<sup>+</sup> counterparts



Table 1. PCR primers

Gene	Direction	Primer
MMP9	Forward	5'-CTCGAACTTTGACAGCGACA-3'
	Reverse	5'-GCCATTACGTCGTCCTTAT-3'
MMP2	Forward	5'-ACCCAGATGTGGCCAACTAC-3'
	Reverse	5'-TCATGATGTCTGCCTCTCCA-3'
18S	Forward	5'-AAACGGCTACCACATCCAAG-3'
	Reverse	5'-CCTCCAATGGATCCTCGTTA-3'

were labeled with iTRAQ reagents 115 (case 1) or 117 (case 2). Labeled peptide samples were mixed and fractionated as described previously.<sup>23</sup>

### Mass spectrometric analysis

NanoLC-MS/MS analyses were performed on an LTQ-Orbitrap XL (Thermo Fisher Scientific, Waltham, MA) equipped with a nano-ESI source and coupled to a Paradigm MG2 pump (Michrom Bioresources, Auburn, CA) and autosampler (HTC PAL, CTC Analytics, Zwingen, Switzerland).<sup>23</sup>

### iTRAQ data analysis

Protein identification and quantitation for iTRAQ analysis was carried out using SEQUEST (Bioworks version 3.3.1, Thermo Fisher Scientific) searching against the International Protein Index (IPI) human protein database (version 3.26).<sup>23</sup> Relative protein abundances were determined by comparing the ratio of iTRAQ reporter ion intensities in the MS/MS scan.<sup>23</sup>

### Quantitation of CD82-expressing cells using flow cytometry (FACS)

Leukemic peripheral blood (PB) ( $n = 3$ ) and BM ( $n = 9$ ) cells were collected from 12 AML patients (case numbers 1–12) after obtaining informed consent. Leukemic cells were stained with a fluorescein isothiocyanate (FITC)-conjugated monoclonal antibody (mAb) against CD34 (Beckman coulter, CA), a phycoerythrin (PE)-conjugated mAb against CD82 (Abcam, Cambridge, UK), and a PE Cy5-conjugated mAb against CD38 (BioLegend, San Jose, CA). Cells were stained for 30 min on ice. Isotype-matched immunoglobulins were used as controls. Cells were then analyzed using flow cytometry (FACS Calibur, Becton Dickinson, San Jose, CA) following data analysis by FlowJo software (TreeStar, San Carlos, CA).

### RNA isolation and real-time reverse transcription-polymerase chain reaction (RT-PCR)

RNA isolation and cDNA preparation were performed as described previously.<sup>24</sup> Real-time RT-PCR was carried out by using Power SYBR Green PCR Master Mix (Applied Biosystems, Warrington, UK) as described previously.<sup>24</sup> Primers for PCR are shown in Table 1.

### Small interfering RNA

Control small interfering (si) RNA and an siRNA against CD82 were purchased from Santa Cruz Biotechnology and Sigma (Deisenhofen, Germany), respectively.

### Transfections

EOL-1 and EOL-1R cells were transiently transfected with either control or CD82 siRNA (300 nM) using an Amaxa Nucleofector II electroporator (Wako Pure Chemical Industries, Ltd., Osaka, Japan) with a Nucleofector Kit V (program U-001) as previously described.<sup>25</sup> The preliminary experiments using the green fluorescence protein-expressing vector found that efficacy of transfection with this program was approximately 70% with nearly 70% cell viability, as measured by FACS and Annexin V/PI staining, respectively (figure not shown).

### CD82 shRNA lentiviral vector, production and infection

The short hairpin (sh) RNA sequence used to target human CD82 corresponded to the following sequence on the human CD82 transcript variant 2, NCB I accession number NM\_001024844. Lentiviral shRNA particles were produced using the viral power packaging system (Invitrogen, CA) with the 293FT packaging cell line (Invitrogen), and lentiviral CD82 shRNA particles ( $>10^8$  titer unit (TU)/ml) were prepared using ultracentrifugation.  $5 \times 10^4$  CD34<sup>+</sup>/CD38<sup>−</sup> AML cells were seeded in 24-well plates in 500  $\mu$ l of Iscove's modified Dulbecco's medium (IMDM) (Invitrogen) containing 10% heat inactivated fetal bovine serum (FBS). After overnight incubation,  $5 \times 10^5$  TU lentiviral CD82 shRNA particles and polybrene (10  $\mu$ g/ml) were added per well with serum free medium containing IMDM. After overnight, 1 ml of full media supplemented with FBS, 2-mercaptoethanol, stem cell factor, granulocyte-macrophage colony-stimulating factor (GM-CSF), granulocyte-colony-stimulating factor (G-CSF), IL-3, and erythropoietin (EPO) was added and incubated for 7 days. The control and CD82 shRNA lentiviral vectors co-expressed green fluorescence protein (GFP). Quantification of GFP-positive cells using FACS analysis indicated that the lentiviral transduction efficiency was nearly 70% (Supporting Information Fig. S1b). GFP-positive cells were sorted using JSAN (Bay bioscience Co., Ltd., Kobe, Japan).

### CD82 lentiviral vector

CD82 cDNA was purchased from Mammalian gene collection (BC000726) and was used as the template for PCR. PCR products were cloned into pLenti6.3/V5-TOPO vector (Invitrogen). CD82-transfected lentiviral particles were produced using the viral power packaging system (Invitrogen) with the 293FT packaging cell line (Invitrogen). The pLenti6.3/V5-TOPO vector was designed to co-express V5 epitope;  $5 \times 10^4$  CD34<sup>+</sup>/CD38<sup>+</sup> AML cells were seeded in 24-well plates in 500  $\mu$ l of IMDM (Invitrogen) containing 10% FBS. After overnight incubation,  $5 \times 10^5$  TU lentiviral CD82-transfected

lentiviral particles and polybrene (10 µg/ml) were added per well. After overnight, supernatant was removed and 1 ml of full media was added and incubated for 7 days. FACS analysis utilizing an anti-V5 antibody (Invitrogen, R960-25) indicated that the efficiency of transduction into CD34<sup>+</sup>/CD38<sup>+</sup> AML cells was nearly 80% (Supporting Information Fig. S1b).

### Migration assays

Freshly isolated either CD34<sup>+</sup>/CD38<sup>-</sup> ( $5 \times 10^5$  cells) or CD34<sup>+</sup>/CD38<sup>+</sup> AML cells ( $1 \times 10^5$  cells) were transduced by either CD82 shRNA or CD82 cDNA, respectively, and then seeded in the upper inserts with 3 µm pores coated by fibronectin (Cat. No. 354543, Becton Dickinson Biosciences, Bedford, MA) and mesenchymal stromal cells (MSCs) established from healthy donors, while the lower wells were filled with Iscove's Modified Dulbecco's Medium (IMDM) containing 10% heat inactivated FBS. Similarly, EOL-1 and EOL-1R cells were transiently transfected with either control or CD82 siRNA. After 48 hr, these cells ( $5 \times 10^5$  cells in 100 µl RPMI-1640) were seeded in the upper biocoat cell culture inserts coated by fibronectin, and the lower well was filled to the top with RPMI-1640 containing 10% heat inactivated FBS as a chemoattractant. After incubation for 48 hr, the supernatant was discarded and the cells that had adhered to the fibronectin were gently washed in phosphate-buffered saline (PBS). Cells were then fixed for 1 hr in 4% paraformaldehyde, washed twice in PBS, stained with 4'-diamidino-2-phenylindole (DAPI), and counted under a microscope (OLYMPUS FV1000-D). The cells that had passed through the membrane filter were collected and the number of viable cells was counted under light microscope after staining with trypan blue.

### Gelatin zymography

The culture supernatant as well as whole cell proteins of EOL-1 and EOL-1R cells were harvested. Gelatinolytic activities were carried out by utilizing a gelatin-zymography kit (Primarycell, Hokkaido, Japan). Each lane was loaded with 30 µg of whole protein lysates or 20 µl of supernatant.

### Colony forming assay

The colony-forming assay was performed with methylcellulose medium H4034 (StemCell Technologies, Vancouver, BC, Canada), as previously described.<sup>20</sup>

### Bone marrow transplantation and engraftment assay

NOD.Cg-Rag1<sup>tm1Mom</sup> Il2rg<sup>tm1Wjl</sup>/SzJ mice (Stock number: 007799) were purchased from the Jackson Laboratory for experimental animals (Bar Harbor)<sup>26</sup> and bred in a pathogen-free environment in accordance with the guidelines of the Kochi University School of Medicine. The 6-week-old mice were utilized for experiments. CD34<sup>+</sup>/CD38<sup>-</sup> AML cells ( $1 \times 10^4$  cells) transduced with either scrambled control or CD82 shRNA were injected to each mouse intravenously *via*

the tail vein. At 9 weeks after transplantation, mice were euthanized and BM were removed. BM cells were flushed from the femurs using 25-gauge needles (Becton Dickinson Biosciences) and then fixed in formalin. The human cell engraftment was analyzed by using flow cytometry after staining of spleen cells with human CD45 PE Cy5-conjugated mAb (Dako, Glostrup, Denmark) and human CD33 PE-conjugated mAb (Becton Dickinson Biosciences).

### Single cell RT-PCR

A single CD34<sup>+</sup>/CD38<sup>-</sup> AML cell was isolated by BD FACS AriaII (Becton Dickinson Biosciences) and subjected to RT-PCR by AmpliSpeed slide cyclor (Beckman Coulter, Munich, Germany) and ABI StepOnePlus (Applied Biosystems) to measure the levels of CD82 and MMP9.

### Immunohistochemistry of CD82 in BM sections

Immunohistochemical staining of CD82 was performed with a Ventana DISCOVERY<sup>TM</sup> autostainer system (Ventana Japan, Osaka, Japan) as previously described.<sup>25</sup> The anti-CD82 antibody (Santa Cruz Biotechnology, Santa Cruz, CA) was used.

### Cell cycle analysis by flow cytometry (FACS)

Cell cycle distribution of CD34<sup>+</sup>/CD38<sup>-</sup> AML cell was measured as previously described after transduction of either scrambled control or CD82 shRNA. Briefly, the cells were stained with Ki-67 (Santa Cruz Biotechnology) and propidium iodide and subjected to FACS.<sup>20</sup>

### Homing analysis

The human AML cells isolated from patients were treated with anti-human CD82 (Santa Cruz Biotechnology) or control IgG (eBiosScience, San Diego, CA) antibody on ice for 1 hr. This anti-CD82 antibody worked as a neutralizing antibody (Nishioka *et al.* unpublished data). Cells were washed gently with PBS and were injected to each mouse intravenously *via* the tail vein. At 16 hr after transplantation, mice were euthanized and BMs were removed and analyzed by flow cytometry with anti-human CD45 and CD34 antibodies. We acquired in the range of  $1 \times 10^6$  to  $3 \times 10^6$  events per sample.

### Statistical analysis

When comparing two groups, Student's *t*-test was used. For demonstration of association, the Pearson's correlation coefficient test was applied. All statistical analyses were carried out using SPSS software (Version 11.03; spss, Tokyo, Japan) and the results were considered to be significant when the *p* value was <0.05, and highly significant when the *p* value was <0.01.

## Results

### Protein expression profiles of CD34<sup>+</sup>/CD38<sup>-</sup> AML cells and CD34<sup>+</sup>/CD38<sup>+</sup> counterparts

Four samples (two from CD34<sup>+</sup>/CD38<sup>-</sup> AML cells lysates and two from CD34<sup>+</sup>/CD38<sup>+</sup> counterparts lysates, approximately 10 million cells per sample) were trypsinized and



Table 2. Protein expression profiles of CD34<sup>+</sup>/CD38<sup>−</sup> and CD34<sup>+</sup>/CD38<sup>+</sup> AML cells

NCBI accession no.	Protein	Average iTRAQ ration (114/115)	Average iTRAQ ration (116/117)	Gene symbol
P27701	Adhesion: CD82 antigen	4.64	3.79	CD82 (KAI1)
Q9H165	Apoptosis: Isoform 1 of B-cell lymphoma/leukemia 11A	5.79	6.38	BCL11A (CTIP1)
P47738	Enzyme: Aldehyde dehydrogenase, mitochondrial precursor	5.22	4.43	ALDH
Q9H0C8	Enzyme: Integrin-linked kinase-associated serine/threonine phosphatase 2C	4.29	10.52	ILKAP
P01903	Immunity: HLA class II histocompatibility antigen, DR alpha chain precursor	6.11	3.87	HLA-DRA

labeled with a specific isobaric iTRAQ reagent. To compensate for extreme sample complexity, each iTRAQ sample was separated into 24 fractions using strong cation-exchange chromatography.<sup>23</sup> A total of 2,537 and 2,506 proteins were identified with >95% confidence for each of the biological replicates. Since iTRAQ internal replicates typically yield high confidence results,<sup>27</sup> differences greater than threefold or less than 0.5-fold are considered significant. We listed the proteins whose expression was greater than 3-fold or less than 0.5-fold in CD34<sup>+</sup>/CD38<sup>−</sup> AML cells as compared with their CD34<sup>+</sup>/CD38<sup>+</sup> counterparts in Table 2 and Supporting Information Table 2. Either 481 or 700 proteins were differentially expressed in case 1 and case 2, respectively (Table not shown), and only 104 proteins were overlapped in both cases (Table 2, Supporting Information Table S1). The expression of 98 of these proteins increased, while the expression of six proteins decreased in both cases (Table 2, Supporting Information Table S1). Two of the identified proteins are involved in differentiation, two play a role in the cell cycle, six play a role in adhesion, five are involved in DNA replication and repair, and eight are involved in apoptosis and anti-apoptosis (Table 2, Supporting Information Table S1). In addition, 6 nuclear transcription factors, 17 enzymes involved in drug-resistance, 6 human leukocyte antigens, 18 ribosome nucleoproteins, and 10 histone and histone-binding proteins were differentially expressed between CD34<sup>+</sup>/CD38<sup>−</sup> AML and CD34<sup>+</sup>/CD38<sup>+</sup> counterparts (Supporting Information Table S1). Additional differentially expressed proteins are also listed in Supporting Information Table S1. Other studies identified aldehyde dehydrogenase activity (ALDH), B-cell lymphoma/leukemia 11A (BCL11A), ILK, and HLA-DR as highly expressed proteins in leukemia stem cells.<sup>28–31</sup> These proteins were also overexpressed in CD34<sup>+</sup>/CD38<sup>−</sup> AML cells in the present study (Table 2), indicating an acceptable sensitivity of the current study.

CD82 is overexpressed in CD34<sup>+</sup>/CD38<sup>−</sup> AML cells

We focused on CD82 because this protein functions as an adhesion molecule that is important to maintain the character of LSCs. We attempted to validate these results in other

CD34<sup>+</sup>/CD38<sup>−</sup> AML cells isolated from patients (11 from BM, 5 from PB, cases 1–14, 17, 18) by FACS. In 15 of 16 cases (94%), the relative expression levels of CD82 were significantly higher in CD34<sup>+</sup>/CD38<sup>−</sup> AML cells (68 ± 27%) as compared with their CD34<sup>+</sup>/CD38<sup>+</sup> counterparts (30 ± 19%) (*p* < 0.01, Fig.1a, Supporting Information Fig. S2a). On the other hand, a mean 35 ± 19% of CD34<sup>+</sup> hematopoietic stem/progenitor cells isolated from healthy volunteers (*n* = 6) were positive for CD82 staining (Supporting Information Fig. S2b). In addition, we found that imatinib-resistant EOL-1R cells which stayed on a dormant state and possessed the immature character with aberrant expression of CD34 (data not shown) expressed a greater amount of CD82 on their cell surface (96 ± 1%) than parental EOL-1 cells (47 ± 4%) (Fig. 1a).

The MMPs enzymatic activity

Aberrant expression of CD82 was associated with inactivation of matrix metalloproteinase 9 (MMP9) in the H1299 human lung carcinoma cells.<sup>14</sup> We therefore examined the relationship between CD82 and MMPs in CD34<sup>+</sup>/CD38<sup>−</sup> AML cells. Real-time RT-PCR found that the levels of MMP9 were significantly lower in CD82 over-expressed CD34<sup>+</sup>/CD38<sup>−</sup> AML cells than their CD34<sup>+</sup>/CD38<sup>+</sup> counterparts (*n* = 7, *p* < 0.01) (Fig. 1b). On the other hand, levels of MMP2 in CD34<sup>+</sup>/CD38<sup>−</sup> AML cells were almost identical to those in CD34<sup>+</sup>/CD38<sup>+</sup> counterparts (Fig. 1b). We also found that the levels of both MMP-9 and -2 were down-regulated in imatinib-resistant EOL-1R cells as compared with parental EOL-1 cells (Fig. 1b). To explore a potential link between CD82 and MMPs in leukemia cells, EOL-1R cells were transiently transfected with either scrambled control or CD82 siRNA (Fig. 1c), which efficiently decreased levels of CD82 in these cells (from 96 ± 1% to 41 ± 1%, Fig. 1c). The MMPs enzymatic activity in these cells was determined by performing gelatin zymography with the culture supernatant as well as whole cell proteins extracted from EOL-1 and EOL-1R cells (Fig. 1d). Interestingly, when CD82 was down-regulated in EOL-1R cells by an siRNA, enzymatic activity of MMP9 was dramatically increased (Fig. 1d), suggesting that CD82 negatively regulated MMP9. Real-time RT-PCR found that

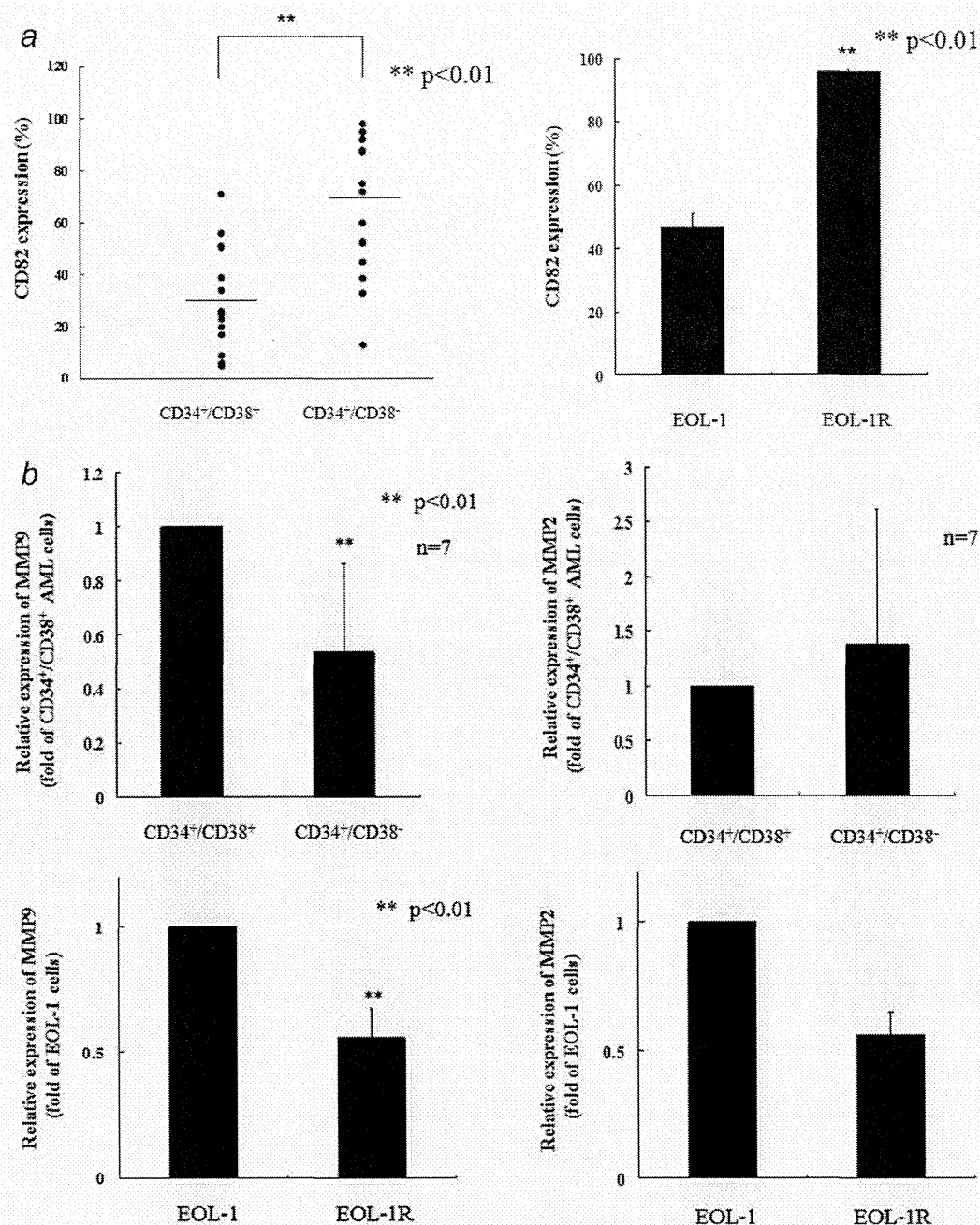


**Figure 1.** CD82 expression in CD34<sup>+</sup>/CD38<sup>-</sup> AML cells and CD34<sup>+</sup>/CD38<sup>+</sup> counterparts. (a) Leukemia cells isolated from patients (BM,  $n = 11$ ; PB,  $n = 5$ ) were stained with anti-CD34, -CD38, and -CD82 antibodies. Expression of CD82 in CD34<sup>+</sup>/CD38<sup>-</sup> AML cells and their CD34<sup>+</sup>/CD38<sup>+</sup> counterparts was analyzed using FlowJo. Each dot represents expression of CD82 for an individual and the mean value is indicated by the line. EOL-1 or EOL-1R cells were stained with anti-CD82 antibody. Expression of CD82 in EOL-1 or EOL-1R cells was analyzed using FlowJo. Statistical significance was determined by paired *t*-test.  $^{**}p < 0.01$ , with respect to control. The effect of CD82 on MMPs. Real-time RT-PCR. (b) RNA was extracted from EOL-1, EOL-1R, and CD34<sup>+</sup>/CD38<sup>-</sup> cells and their CD34<sup>+</sup>/CD38<sup>+</sup> counterparts isolated from AML patients. cDNAs were synthesized and subjected to real-time RT-PCR to measure the levels of MMP9 and MMP2. Results represent the mean  $\pm$  SD of three experiments performed in triplicate. The statistical significance was assessed by a paired *t*-test.  $^{**}p < 0.01$ ;  $^{*}p < 0.05$ . FACS. (c) EOL-1 cells were transiently transfected with either scrambled control or CD82 siRNA. After 24 hr, cells were subjected to FACS to quantify the proportion of CD82-expressing cells. Gelatin zymography. (d) EOL-1 and EOL-1R cells were transfected with either scrambled control or CD82 siRNA. After 48 hr, whole cell lysates and culture supernatant were collected. The enzymatic activity of MMPs was determined by a gelatin-zymography kit, following the manufacturer's instructions. Real-time RT-PCR. (e) EOL-1R cells were transfected with either scrambled control or CD82 siRNA. After 24 hr, these cells were collected and mRNAs were extracted. cDNAs were synthesized and subjected to real-time RT-PCR to measure the levels of MMP9 and MMP2. Results represent mean  $\pm$  SD of duplicate cultures.  $^{**}p < 0.01$ ;  $^{*}p < 0.05$ . FACS. (f) CD34<sup>+</sup>/CD38<sup>-</sup> AML cells (cases 1, 2, 6, and 14) were transduced with either control or CD82 shRNA. (h) CD34<sup>+</sup>/CD38<sup>+</sup> AML cells (cases 1, 2, 14, and 15) were transduced with either empty vector or CD82-expressing lentiviral particles. These cells were subjected to FACS to quantify the proportion of CD82-expressing cells. Real-time RT-PCR. (g) CD34<sup>+</sup>/CD38<sup>-</sup> (cases 1, 2, and 6) or (i) CD34<sup>+</sup>/CD38<sup>+</sup> AML cells (cases 1, 2, 14, and 15) transduced with CD82 shRNA or CD82-expressing lentiviral particles were collected and mRNAs were extracted. cDNAs were synthesized and subjected to real-time RT-PCR to measure the levels of MMP9. Each dot represents the levels of MMP9 for an individual experiment and the mean is indicated by the line.  $^{**}p < 0.01$ ;  $^{*}p < 0.05$ .

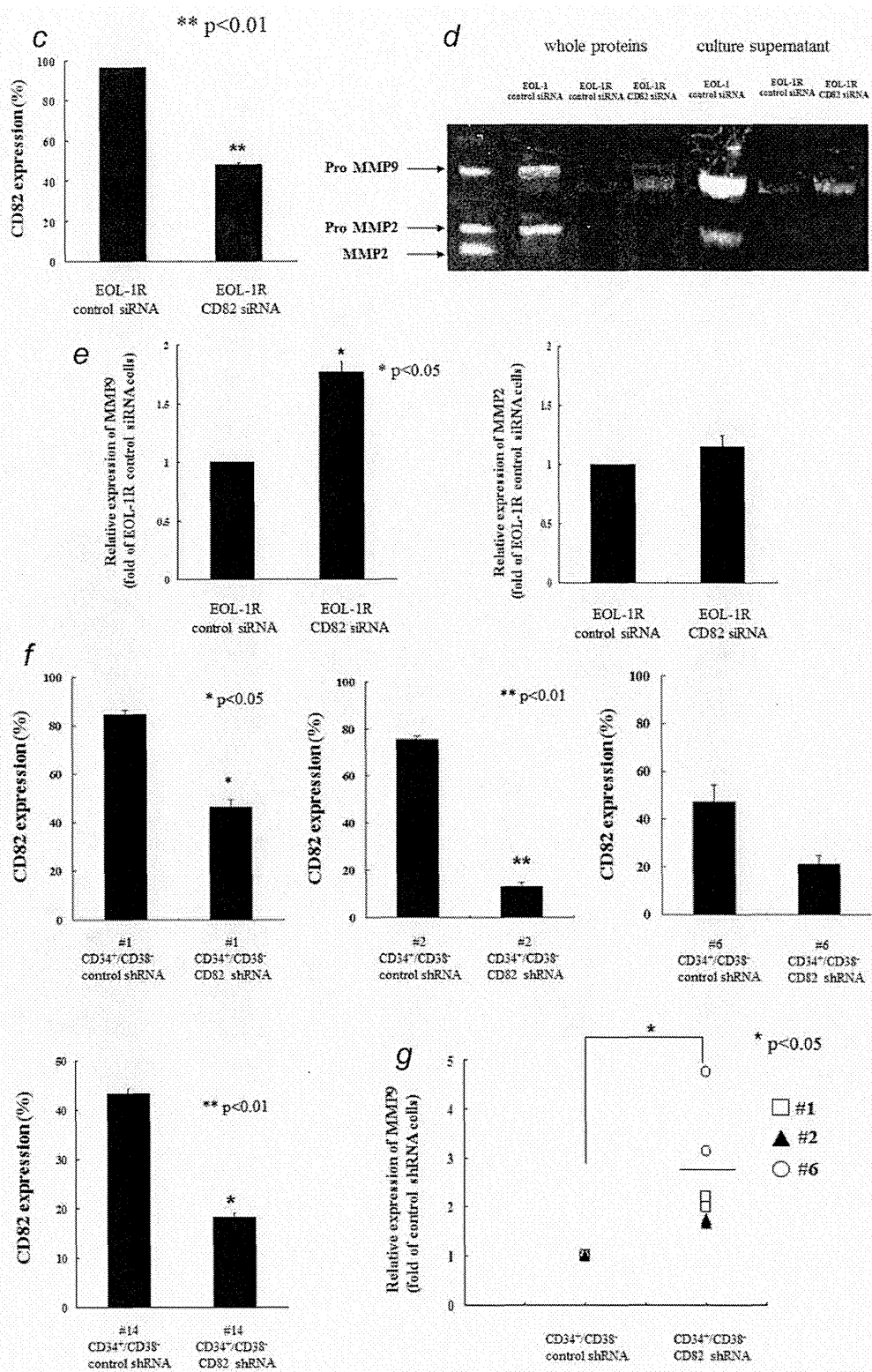


Figure 1. (Continued)

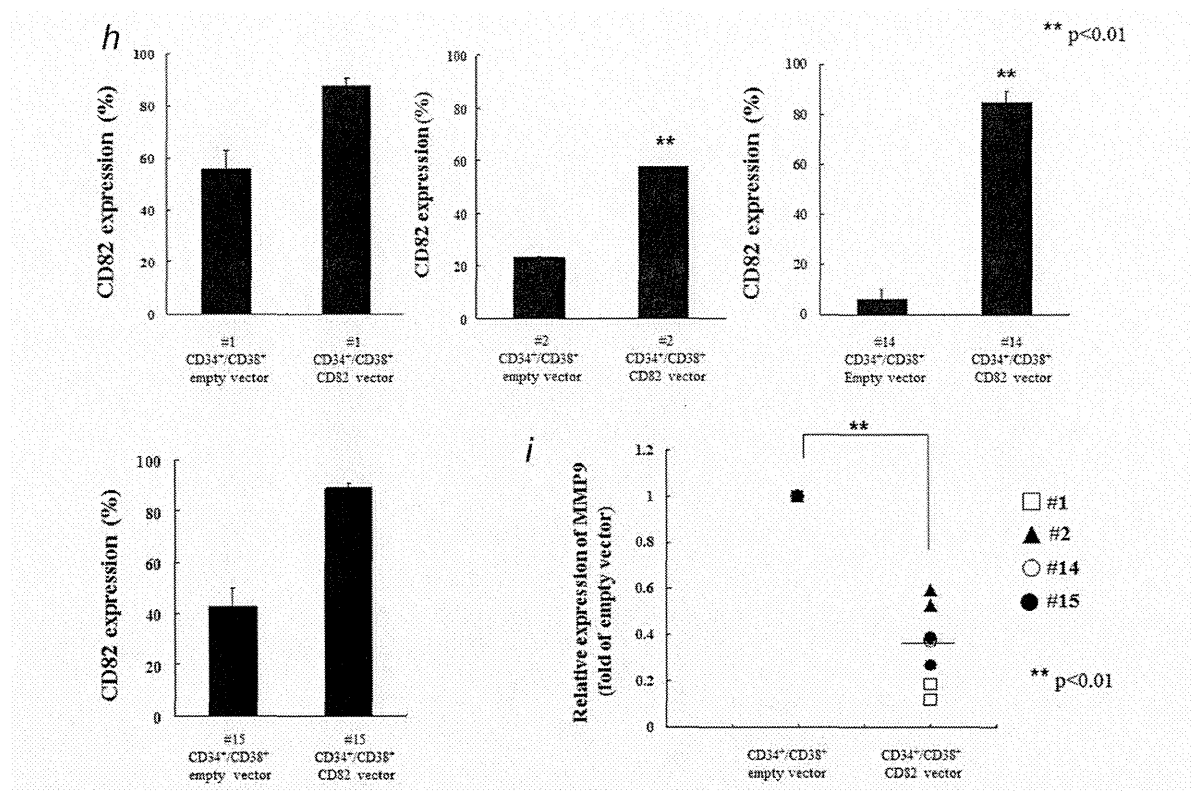


Figure 1. (Continued)

down-regulation of CD82 by an siRNA increased levels of MMP9 by nearly twofold in EOL-1R cells (Fig. 1e). On the other hand, levels of MMP2 were not affected by down-regulation of CD82 (Fig. 1e). Moreover, to explore the function of CD82 in freshly isolated CD34<sup>+</sup>/CD38<sup>-</sup> AML cells, we genetically down-regulated CD82 in these cells. An shRNA targeting CD82 decreased expression of CD82 in four cells (case 1, from  $85 \pm 2\%$  to  $47 \pm 3\%$ ; case 2, from  $75 \pm 1\%$  to  $13 \pm 2\%$ ; case 6, from  $47 \pm 7\%$  to  $21 \pm 3\%$ ,  $p = 0.066$ ; case 14, from  $43 \pm 1\%$  to  $18 \pm 1\%$ , Fig. 1f). Real-time RT-PCR found that the levels of MMP9 were significantly increased after down-regulation of CD82 in CD34<sup>+</sup>/CD38<sup>-</sup> AML cells ( $n = 3$ , cases 1, 2, and 6,  $p < 0.05$ , Fig. 1g). We next exposed CD34<sup>+</sup>/CD38<sup>+</sup> AML cells to the CD82-expressing lentiviral particles, which increased levels of CD82 ( $n = 4$ , case 1; from  $56 \pm 7\%$  to  $88 \pm 3\%$ , case 2, from  $23 \pm 1\%$  to  $58 \pm 1\%$ ; case 14; from  $6 \pm 4\%$  to  $85 \pm 4\%$ , case 15; from  $43 \pm 7\%$  to  $89 \pm 2\%$ , Fig. 1h). As expected, the levels of MMP9 were decreased by half in these cells (Fig. 1i).

#### The effects of CD82 on migration of CD34<sup>+</sup>/CD38<sup>-</sup> AML cells

We next examined the function of CD82 in CD34<sup>+</sup>/CD38<sup>-</sup> AML cells. When levels of CD82 were down-regulated in CD34<sup>+</sup>/CD38<sup>-</sup> AML cells after lentiviral transduction of CD82 shRNA ( $n = 4$ , cases 1, 2, 6 and 14, Fig. 1f), their

migration was significantly stimulated (Fig. 2a). Moreover, we enhanced expression of CD82 in CD34<sup>+</sup>/CD38<sup>+</sup> AML cells by using CD82-expressing lentiviral particles ( $n = 3$ , cases 1, 14 and 15, Fig. 1h). Forced-expression of CD82 in CD34<sup>+</sup>/CD38<sup>+</sup> AML cells dramatically increased number of cells adhered to the insert in parallel with a decrease in the number of migrated cells (Fig. 2b). Similarly, after down-regulation of CD82 in EOL-1R cells, adhesive cells decreased by approximately half (Fig. 2c). In parallel, population of EOL-1R cells migrated to the lower well increased by 10-fold after down-regulation of CD82 in these cells (Fig. 2c).

#### The effect of CD82 on colony forming ability of CD34<sup>+</sup>/CD38<sup>-</sup> AML cells

We first examined whether CD82 regulated proliferation of CD34<sup>+</sup>/CD38<sup>-</sup> AML cells (cases 1, 6, and 14) by using colony forming assay (Fig. 3a). Down-regulation of CD82 by an shRNA (from 59 to 27%) inhibited their colony forming ability by approximately 50% (Fig. 3a). Likewise, down-regulation of CD82 by an siRNA (from 96% to 48%) inhibited colony forming ability of CD34<sup>+</sup> EOL-1R cells which mimic LSCs by mean 50% (Fig. 3b). On the other hand, forced-expression of CD82 in CD34<sup>+</sup>/CD38<sup>+</sup> AML cells (cases 1 and 14) by transduction of CD82-expressing lentiviral particles increased levels of CD82 from 18 to 89% and stimulated their colony forming ability by mean 1.7-fold (Fig. 3c).

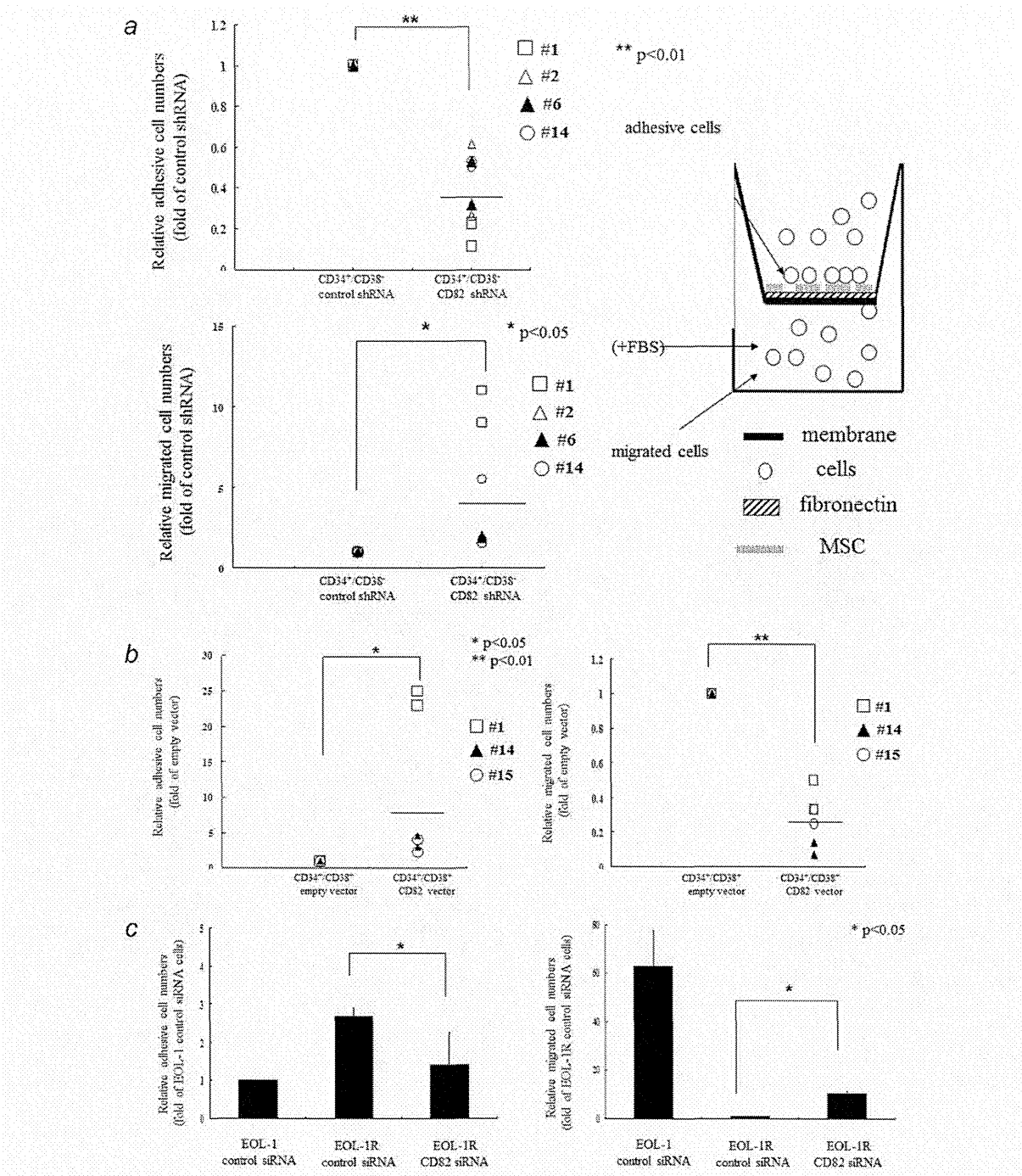


**Figure 2.** The effects of CD82 on migration of leukemia cells. Migration assays. (a) CD34<sup>+</sup>/CD38<sup>-</sup> (cases 1, 2, 6, and 14) or (b) CD34<sup>+</sup>/CD38<sup>+</sup> AML cells (cases 1, 14, and 15) transduced with CD82 shRNA or CD82-expressing lentiviral particle were seeded in the upper biocoat cell culture inserts. After 48 hr, the cells that had migrated through the filters were stained with 4'6-diamidino-2-phenylindole, and counted under a microscope. Each dot represents relative adhesion or migration cell numbers for an individual experiment and the mean is indicated by the line. (c) EOL-1 and EOL-1R cells transfected with either scrambled control or CD82 siRNA were seeded in the upper biocoat cell culture inserts. After 48 hr, the cells that had migrated through the filters were stained with 4'6-diamidino-2-phenylindole, and counted under a microscope. Results represent the mean  $\pm$  SD of two experiments performed in triplicate cultures. \*\* $p < 0.01$ ; \* $p < 0.05$ .

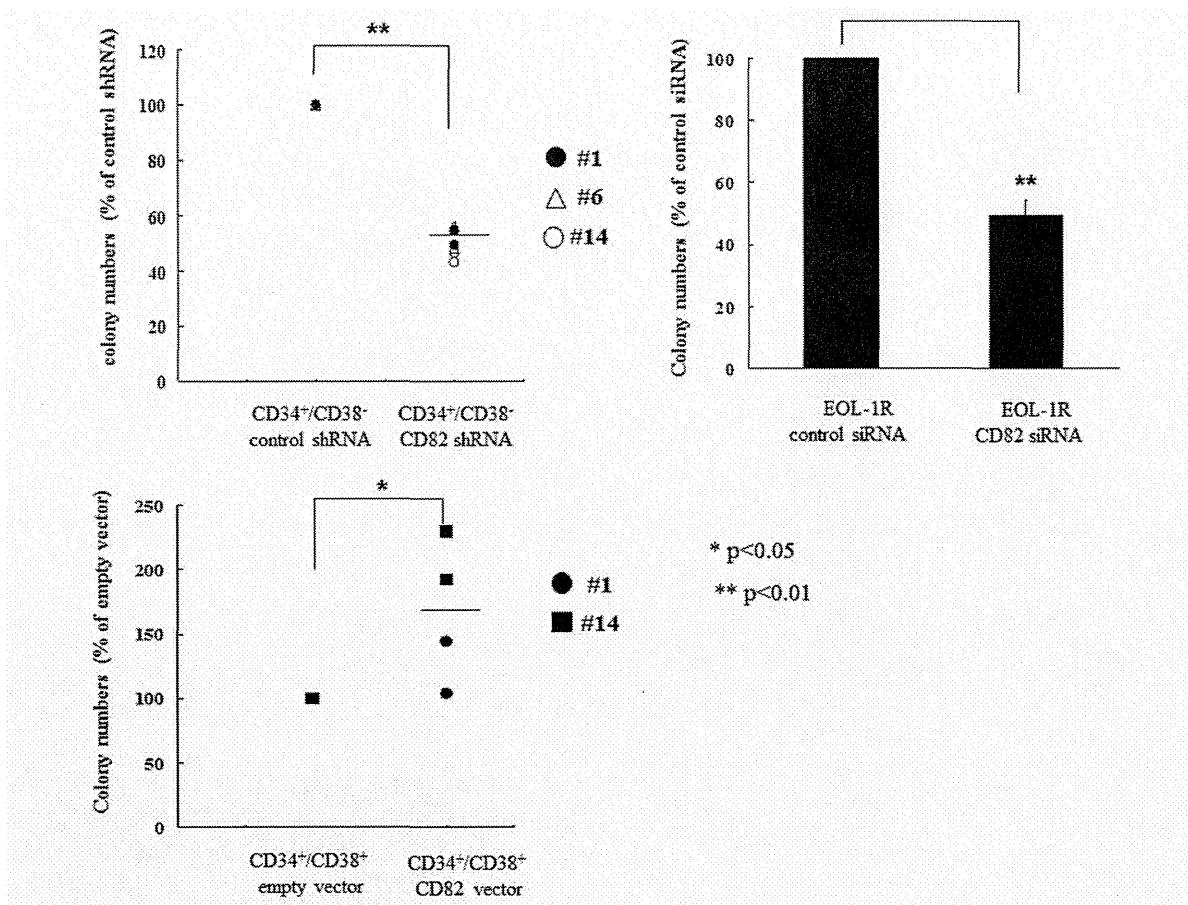


**Figure 3.** The effect of CD82 on proliferation of CD34<sup>+</sup>/CD38<sup>-</sup> AML cells. Colony forming assay. (a) CD34<sup>+</sup>/CD38<sup>-</sup> (cases 1, 6, and 14) or (c) CD34<sup>+</sup>/CD38<sup>+</sup> AML cells (cases 1 and 14) were transduced with CD82 shRNA or CD82-expressing lentiviral particles. (b) EOL-1R cells were transiently transfected with either control or CD82 siRNA. These cells were cultured in methylcellulose medium. After 16 days, colonies were counted. Each dot represents % of colony number compared with control for an individual experiment and the mean is indicated by the line.

These observations suggested that CD82 plays a role in survival of CD34<sup>+</sup>/CD38<sup>-</sup> AML cells.

#### AML engraftment was inhibited by down-regulation of CD82 *in vivo*

We next examined the function of CD82 *in vivo*. CD34<sup>+</sup>/CD38<sup>-</sup> cells isolated from three different AML patients (cases 1, 6 and 14) were transduced with either scrambled control or CD82 shRNA. We transplanted these cells into NOD.Cg-Rag1<sup>tm1Mom</sup> Il2rg<sup>tm1Wjl</sup>/Sz mice *via* the tail vein. Transplanted mice were sacrificed at 9 weeks after transplantation and analyzed the human engraftment in their spleens and BM by quantifying the population of positive cells for human CD45 and CD33 antigens (Figs. 4a and 4b). Transplantation of CD34<sup>+</sup>/CD38<sup>-</sup> AML cells transduced by scrambled control shRNA resulted in the mean human engraftment either 14 ± 6% or 15 ± 5% in spleen and BM, respectively (n = 8, Fig. 4a). These cells expressed CD33anti-

gen on their cell surface (4% in both spleen and BM) (Fig. 4b). On the other hand, when these cells were transduced with CD82 shRNA, human engraftment was significantly impaired (7 ± 4% or 6 ± 2% in spleen and BM, respectively, p < 0.01) (n = 6, Fig. 4a). In addition, population of cells expressing CD33 on their cell surface was decreased to either 0.1% or 1% in spleen and BM, respectively (Fig. 4b). These observations suggested that down-regulation of CD82 impaired AML engraftment as well as AML reconstitution in an immunodeficient mice. In addition, we assessed levels of CD82 and MMP9 in isolated CD34<sup>+</sup>/CD38<sup>-</sup> AML cells (n = 9) by using single cell real-time RT-PCR (Fig. 4c). Inverse correlation was noted between levels of CD82 and MMP9 (r = -0.58, Fig. 4c). Moreover, we examined the levels of CD82 in transplanted human AML cells as well as localization of these cells in murine BM by immunohistochemistry (Figs. 4d-4g). Notably, human AML cells expressing CD82 were localized in endosteal region of BM at 9 weeks after



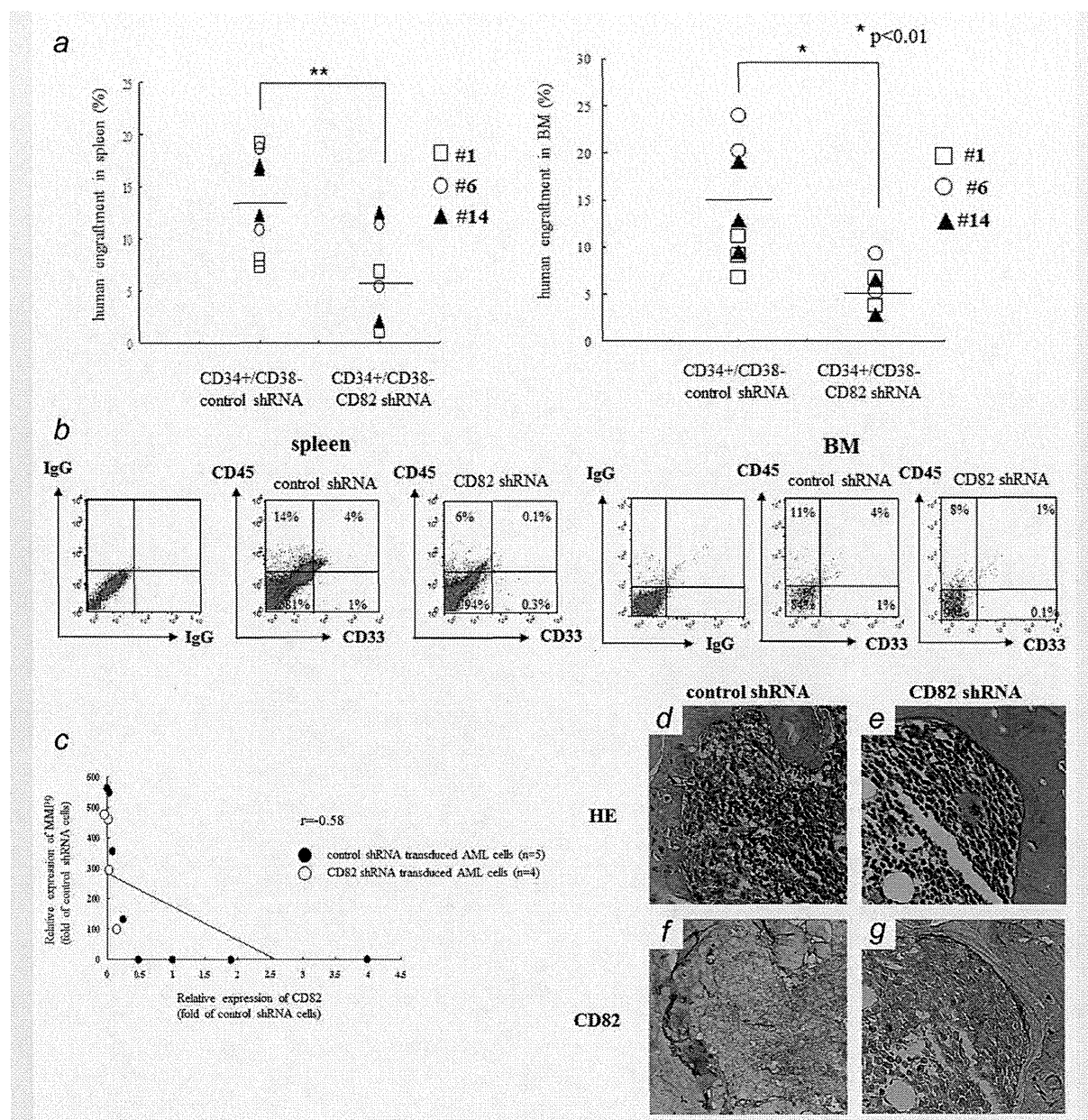


**Figure 4.** Down-regulation of CD82 impairs the AML engraftment. CD34<sup>+</sup>/CD38<sup>-</sup> AML cells were isolated from three AML patients (cases 1, 6, and 14) and transduced with either scrambled control or CD82 shRNA. These cells were transplanted into NOD.Cg-Rag1<sup>tm1Mom</sup> Il2rg<sup>tm1Wjl</sup>/Sz mice via the tail vein. At 9 weeks after transplantation, mice were euthanized and then spleen were removed. AML engraftment. (a) The percentages of human CD45 were analyzed to monitor the human engraftment in murine spleen and BM (scrambled control shRNA; n = 8, CD82 shRNA; n = 6) by using flow cytometry. Each dot represents CD45 expression for an individual experiment and the mean is indicated by the line. FACS. (b) Spleen and BM cells isolated from NOD.Cg-Rag1<sup>tm1Mom</sup> Il2rg<sup>tm1Wjl</sup>/Sz mice received transplantation of CD34<sup>+</sup>/CD38<sup>-</sup> AML cells (cases 1, 6, and 14) transduced with either CD82 shRNA or control shRNA were stained with anti-human CD45 and CD33 antibodies. Representative flow cytometric analyses of human CD45 and CD33 expression in murine spleen and BM cells are shown. Relationship between MMP9 and CD82. (c) A single CD34<sup>+</sup>/CD38<sup>-</sup> AML cell was isolated from murine BMs by BD FACS ARIAII. These cells were subjected to reverse transcription by AmpliSpeed slide cycle and the synthesized cDNA was subjected to real-time PCR to measure the levels of CD82 and MMP9. Results showed relative expression of MMP9 versus that of CD82. For demonstration of association, the Pearson's correlation coefficient test was applied. ● Scrambled control shRNA; n = 5, ○ CD82 shRNA; n = 4. Immunohistochemistry. BMs were removed from mice, who were transplanted with either (d, f) scrambled control or (e, g) CD82 shRNA transduced CD34<sup>+</sup>/CD38<sup>-</sup> AML cells. These BMs were stained with either (d, e) hematoxylin and eosin (HE) or (f, g) an anti-human CD82 antibody (CD82) and examined under light microscope.



transplantation of scrambled control shRNA transduced CD34<sup>+</sup>/CD38<sup>-</sup> AML cells (Figs. 4d and 4f). On the other hand, human AML cells were not detectable in this region of murine BM, that were transplanted with CD82-depleted CD34<sup>+</sup>/CD38<sup>-</sup> AML cells (Figs. 4e and 4g). To examine longer-term reconstituting capability, we carried out secondary transplantation of CD34<sup>+</sup>/CD38<sup>-</sup> AML cells recovered from primary recipient mice. At 9 weeks post-transplantation, human AML engraftment was 18% as assessed by quantification of human CD45 expressing cells in PB isolated from the secondary recipients by FACS. These observations suggested that functional properties of CD34<sup>+</sup>/CD38<sup>-</sup> AML cells were maintained in the BM microenvironment of recipient mice and CD34<sup>+</sup>/CD38<sup>-</sup> AML cells utilized in this study fulfill the criteria for LSCs *in vivo*.

Moreover, we examined whether CD82 affected homing of AML cells to BM. AML cells isolated from three patients (cases 6, 14, 17) were treated with anti-CD82 or control IgG antibody. These cells were transplanted per mouse, and homing of the cells was analyzed in the BM of mice after 16 hr of transplantation. In the control group ( $n = 6$ ), an average of 0.39% in human CD34<sup>+</sup> AML cells were detected in the mouse BM compared with 0.77% in the CD82 antibody-treated group (Supporting Information Fig. S6).

## Discussion

Previous studies showed that the LSCs-niche interaction was important to maintain the stemness of leukemia cells.<sup>15</sup> In this study, iTRAQ technique identified adhesion molecule CD82 as an overexpressed protein in CD34<sup>+</sup>/CD38<sup>-</sup> AML cells (Supporting Information Table S1). Additional experiments utilizing FACS confirmed aberrant expression of CD82 in freshly isolated CD34<sup>+</sup>/CD38<sup>-</sup> AML cells ( $n = 16$ ) (Fig. 1a). In addition, this study found that down-regulation of CD82 by an shRNA increased levels of MMP9 in CD34<sup>+</sup>/CD38<sup>-</sup> AML cells (Fig. 1g) and stimulated their migration (Fig. 2a). Meanwhile, forced expression of CD82 decreased levels of MMP9 mRNA in CD34<sup>+</sup>/CD38<sup>+</sup> AML cells (Fig. 1i) and enhanced adhesion of these cells to fibronectin and MSCs, a kind of artificial BM niche (Fig. 2b). Single cell RT-PCR also demonstrated that down-regulation of CD82 by an shRNA increased levels of MMP9 mRNA in CD34<sup>+</sup>/CD38<sup>-</sup> AML cells, and reverse correlation was noted between levels of MMP9 and CD82 in CD34<sup>+</sup>/CD38<sup>-</sup> AML cells (Fig. 4c). The levels of MMP9 mRNA in CD34<sup>+</sup>/CD38<sup>-</sup> AML cells shown in Figures 1g and 4c were inconsistent, although the cells utilized in these studies were isolated from same populations. In these studies shown in Figure 4c, we used a single cell immediately after isolation from murine BM. On the other hand, cells used in these studies shown in Figure 1g were incubated for 7 days in full media to be transduced by shRNA. As a result, the levels of MMP9 mRNA in leukemia cells might be down-regulated in these cells. Notably, down-regulation of CD82 in CD34<sup>+</sup>/CD38<sup>-</sup> AML cells ( $n = 3$ ) by an shRNA impaired engraftment of these cells in the BM as

well as spleen in NOD.Cg-*Rag1*<sup>tm1Mom</sup> *Il2rg*<sup>tm1Wjl</sup>/SzJ mice (Fig. 4a). These observations suggested that CD82 played an important role in adhesion of CD34<sup>+</sup>/CD38<sup>-</sup> AML cells to BM microenvironment *via* down-regulation of MMP9. Other investigators showed that MMP9 in human mononuclear phagocytes was inhibited by IL-10.<sup>32</sup> Similarly, IL-10 activated the tissue inhibitors of expression of metalloproteinases (TIMP-1/2) and down-regulated the levels of MMP2 and MMP9 in human prostate cancer cells.<sup>33</sup> Thus, down-regulation of MMP9 by IL-10 may augment adhesion of HSCs to BM osteoblastic niche and exogenous administration of IL-10 may be useful to promote the repopulating ability of HSCs and engraftment of HSCs to BM niche. We also found that exposure of CD34<sup>+</sup>/CD38<sup>-</sup> AML cells to IL-10 (5 ng/ml) down-regulated levels of MMP9 mRNA in these cells (Supporting Information Fig. S5). On the other hand, down-regulation of IL-10 in these cells ( $n = 2$ , cases 2 and 6) by an shRNA increased levels of MMP9 by twofold (Supporting Information Fig. S5). Further experiments found that down-regulation of CD82 in CD34<sup>+</sup>/CD38<sup>-</sup> AML cells by an shRNA potently down-regulated levels of IL-10 (in preparation for publication). Notably, forced expression of CD82 down-regulated levels of MMP9 mRNA, resulting in inactivation of MMP9 in leukemia cells (Figs. 1d and 1e). We therefore hypothesize that CD82 may inactivate MMP9 *via* IL-10 signaling in LSCs. MMP9 promotes mobilization of HSCs from the BM osteoblastic niche by release of soluble Kit-ligand (sKitL),<sup>34</sup> which increases the motility of HSCs and progenitors within the BM. In addition, MMPs cleave integrin  $\beta 4$  and  $\beta 1$  in cultured human corneal epithelial cells and mouse epidermal keratinocytes.<sup>35</sup> CD82 associates with various integrins including  $\alpha 3\beta 1$ ,  $\alpha 4\beta 1$  and  $\alpha 6\beta 1$ .<sup>36,37</sup> Amongst them integrin  $\alpha 4\beta 1$  (VLA4) plays an important role in adhesion of LSCs to BM microenvironment.<sup>38</sup> We found that CD34<sup>+</sup>/CD38<sup>-</sup> AML cells expressed a greater amount of integrin  $\alpha 4\beta 1$  (VLA4) than their counterparts, as measured by real time RT-PCR ( $n = 5$ , Supporting Information Fig. S7a). The hematopoietic cells adhere to stromal endothelial cells through the VLA4/vascular cellular adhesion molecule-1 (VCAM-1) pathway.<sup>39</sup> Thus, activation of MMP9 by down-regulation of CD82 may be able to mobilize CD34<sup>+</sup>/CD38<sup>-</sup> AML cells from BM *via* disruption of interaction between VLA4 and VCAM-1 on cell surface of stromal cells. Moreover, to assess if CD82 interacts with VLA4 molecules, we utilized an anti-integrin  $\beta 1$  (CD29) Ab (Beckman coulter, CA, 6603113) which blocks adhesion of leukemia cells to fibronectine. Forced-expression of CD82 stimulated an adhesion of CD34<sup>+</sup>/CD38<sup>+</sup> AML cells (case 15) to the artificial niche, which was hampered when these cells were treated with an anti-integrin  $\beta 1$  Ab (Supporting Information Fig. S7b). Furthermore, we examined interaction between CD82 and integrin  $\alpha 4$  by utilizing Immunoprecipitation assay and found that CD82 directly interacted with integrin  $\alpha 4$  (Supporting Information Fig. S7c). These observations suggested that VLA4 interacted with CD82 and played a role in adhesion of these cells to the artificial niche.

We found that blockade of CD82 on cell surface of AML cells by an antibody stimulated BM homing of CD34<sup>+</sup> AML cells in these mice (Supporting Information Fig. S6). Similar to the present study, other investigators also showed that cord blood (CB) CD34<sup>+</sup> cells treated with stem cell factor enhanced expression of MMP2/MMP9 and increased BM homing of human CB CD34<sup>+</sup> cells in NOD/SCID mice.<sup>40,41</sup> Thus, blockade of CD82 may increase levels of MMP9, resulting in enhanced migration of AML cells into the BM. However, we hypothesize that these cells could not fully adhere to the BM microenvironment and survive to develop AML.

Interestingly, the CXCR4 antagonist AMD3100 effectively mobilized AML cells without inducing their proliferation.<sup>42</sup> Preclinical studies showed that treatment of leukemic mice with a chemotherapeutic agent in combination with AMD3100 resulted in decreased tumor burden and improved their overall survival compared with mice treated with a chemotherapeutic agent alone. These observations provided a proof-of-principle for directing therapy to the critical tethers that promote AML-niche interactions<sup>42</sup> and supported our hypothesis that inhibition of CD82 could mobilize LSCs from BM niche and sensitize these cells to chemotherapeutic agents. Further studies are clearly required to test our hypothesis *in vivo*.

Another idea to sensitize LSCs to chemotherapeutic agents related to stimulation of cell-cycling of dormant LSCs. Recent studies showed that CD34<sup>+</sup>/CD38<sup>-</sup> AML cells were induced to enter the cell cycle by treatment with G-CSF *in vivo*. G-CSF significantly enhanced apoptosis of CD34<sup>+</sup>/CD38<sup>-</sup> AML cells mediated by cell cycle-dependent chemotherapeutic agents and eliminated CD34<sup>+</sup>/CD38<sup>-</sup> AML cells from mice.<sup>43</sup> The additional experiments found that down-regulation of CD82 was not able to stimulate cell cycling of CD34<sup>+</sup>/CD38<sup>-</sup> AML cells (cases 1 and 6) and EOL-1R cells (Supporting Information Fig. S3), suggesting that CD82 was not involved in the maintenance of dormancy in these cells.

CD82 inhibited the receptor tyrosine kinase human mesenchymal-epithelial transition factor (c-Met) activity,<sup>44</sup> which promoted proliferation and migration of cancer cells.<sup>45,46</sup> c-Met was shown to mediate G-CSF-induced mobilization of he-

matopoietic progenitor cells (HPCs) *via* reactive oxygen species (ROS) signaling.<sup>47</sup> Aberrant expression of CD82 in CD34<sup>+</sup>/CD38<sup>-</sup> AML cells may inactivate c-Met and cause engraftment of these cells to BM niche. We found that levels of CD82 in CD34<sup>+</sup> hematopoietic stem/progenitor cells isolated from healthy volunteers ( $n = 6$ ) were lower than those in CD34<sup>+</sup>/CD38<sup>-</sup> AML cells (35% vs. 59%,  $p = 0.02$ , Supporting Information Fig. S4). Importantly, down-regulation of CD82 in CD34<sup>+</sup> hematopoietic stem/progenitor cells by an shRNA did not significantly inhibit their colony forming ability (Supporting Information Fig. S4).

CD82 expression was strongly correlated with the tumor suppressor gene p53.<sup>48</sup> On the other hand, other studies showed that levels of CD82 did not correlate with the expression of p53 in human hepatocellular carcinoma.<sup>49</sup> We also examined the correlation between CD82 and p53 mRNA levels in CD34<sup>+</sup>/CD38<sup>-</sup> AML cells ( $n = 6$ ) and their CD34<sup>+</sup>/CD38<sup>-</sup> counterparts by utilizing real-time RT-PCR and found that the correlation coefficient was 0.54 (figure not shown). Thus, we think that expression of CD82 is not related with p53 in CD34<sup>+</sup>/CD38<sup>-</sup> AML cells.

Overexpressed CD82 in AML cells may render these cells to adhere to BM niche and regulate maintenance of leukemia stem cells within BM niche. On the other hand, down-regulation of CD82 in AML cells may stimulate circulating of these cells from BM niche to PB.

Taken together, our data suggested that CD82 negatively regulated MMP9 and played an important role in CD34<sup>+</sup>/CD38<sup>-</sup> AML cells to adhere to BM microenvironment. In addition, CD82 was involved in survival of CD34<sup>+</sup>/CD38<sup>-</sup> AML cells. CD82 might be an attractive molecular target to eradicate LSCs in AML patients. Further studies are warranted to evaluate the function of CD82 in LSCs *in vivo*.

## Acknowledgements

This work was supported in part by The Kochi University President's Discretionary Grant (to T.I.), Setsuro Fujii Memorial, The Osaka Foundation for Promotion of Fundamental Medical Research (to T.I.) and Certificate of Kochi Shin-kin/Anshin-tomo-no-kai Prize (to C.N.). C.N. is grateful for a JSPS Research Fellowship for Young Scientists from the Japan Society for the Promotion of Science.

## References

- Bonnet D, Dick JE. Human acute myeloid leukemia is organized as a hierarchy that originates from a primitive hematopoietic cell. *Nat Med* 1997;3:730-7.
- Lapidot T, Sirard C, Vormoor J, et al. A cell initiating human acute myeloid leukaemia after transplantation into SCID mice. *Nature* 1994;367:645-8.
- Blair A, Sutherland HJ. Primitive acute myeloid leukemia cells with long-term proliferative ability in vitro and in vivo lack surface expression of c-kit (CD117). *Exp Hematol* 2000;28:660-71.
- Blair A, Hogge DE, Sutherland HJ. Most acute myeloid leukemia progenitor cells with long-term proliferative ability in vitro and in vivo have the phenotype CD34(+)/CD71(-)/HLA-DR-. *Blood* 1998;92:4325-35.
- Clarke MF, Dick JE, Dirks PB, et al. Cancer stem cells-perspectives on current status and future directions: AACR Workshop on cancer stem cells. *Cancer Res* 2006;66:9339-44.
- Ishikawa F, Yoshida S, Saito Y, et al. Chemotherapy-resistant human AML stem cells home to and engraft within the bone-marrow endosteal region. *Nat Biotechnol* 2007;25:1315-21.
- Taussig DC, Miraki-Moud F, Anjos-Afonso F, et al. Anti-CD38 antibody-mediated clearance of human repopulating cells masks the heterogeneity of leukemia-initiating cells. *Blood* 2008;112:568-75.
- Sarry JE, Murphy K, Perry R, et al. Human acute myelogenous leukemia stem cells are rare and heterogeneous when assayed in NOD/SCID/IL2Rγc-deficient mice. *J Clin Invest* 2011;121:384-95.
- Schofield R. The relationship between the spleen colony forming cell and the hematopoietic stem cell. *Blood Cell* 1978;4:7-25.
- Nilsson SK, Haylock DN, Johnston HM, et al. Hyaluronan is synthesized by primitive hematopoietic cells, participates in their lodgment at the endosteum following transplantation, and is involved in the regulation of their proliferation

- and differentiation in vitro. *Blood* 2003;101:856–62.
11. Zhang J, Niu C, Ye L, et al. Identification of the haematopoietic stem cell niche and control of the niche size. *Nature* 2003;425:836–41.
  12. Calvi LM, Adams GB, Weibrecht KW, et al. Osteoblastic cells regulate the haematopoietic stem cell niche. *Nature* 2003;425:841–6.
  13. Tavor S, Petit I, Porozov S, et al. CXCR4 regulates migration and development of human acute myelogenous leukemia stem cells in transplanted NOD/SCID mice. *Cancer Res* 2004;64:2817–24.
  14. Jin L, Hope KJ, Zhai Q, et al. Targeting of CD44 eradicates human acute myeloid leukemic stem cells. *Nat Med* 2006;12:1167–74.
  15. Avigdor A, Goichberg P, Shviti S, et al. CD44 and hyaluronic acid cooperate with SDF-1 in the trafficking of human CD34+ stem/progenitor cells to bone marrow. *Blood* 2004;103:2981–9.
  16. Dong JT, Lamb PW, Rinker-Schaeffer CW, et al. KAI1, a metastasis suppressor gene for prostate cancer on human chromosome 11p11.2. *Science* 1995;268:884–86.
  17. Ruseva Z, Geiger PX, Hutzler P, et al. Tumor suppressor KAI1 affects integrin  $\alpha$ 5 $\beta$ 3-mediated ovarian cancer cell adhesion, motility, and proliferation. *Exp Cell Res* 2009;315:1759–71.
  18. Jee BK, Park KM, Surendran S, et al. KAI1/CD82 suppresses tumor invasion by MMP9 inactivation via TIMP1 up-regulation in the H1299 human lung carcinoma cell line. *Biochem Biophys Res* 2006;342:655–61.
  19. Popov C, Radic T, Haasters F, et al. Integrins  $\alpha$ 2 $\beta$ 1 and  $\alpha$ 11 $\beta$ 1 regulate the survival of mesenchymal stem cells on collagen I. *Cell Death Dis* 2011;2:e186.
  20. Ikezoe T, Yang J, Nishioka C, et al. Inhibition of signal transducer and activator of transcription 5 by the inhibitor of janus kinases stimulates dormant human leukemia CD34(+) /CD38(-) cells and sensitizes them to antileukemia agents. *Int J Cancer* 2011;128:2317–25.
  21. Nishioka C, Ikezoe T, Yang J, et al. Long-term exposure of leukemia cells to multi-targeted tyrosine kinase inhibitor induces activations of AKT, ERK and STAT5 signaling via epigenetic silencing of the PTEN gene. *Leukemia* 2010;24:1631–40.
  22. Werb Z, Vu TH, Rinkenberger JL, et al. Matrix-degrading proteases and angiogenesis during development and tumor formation. *APMIS* 1999;107:11–18.
  23. Serada S, Fujimoto M, Ogata A, et al. iTRAQ-based proteomic identification of leucine-rich alpha-2 glycoprotein as a novel inflammatory biomarker in autoimmune diseases. *Ann Rheum Dis* 2010;69:770–4.
  24. Ikezoe T, Tanosaki S, Krug U, et al. Insulin-like growth factor binding protein-3 antagonizes the effects of retinoids in myeloid leukemia cells. *Blood* 2004;104:237–42.
  25. Ikezoe T, Takeuchi T, Yang J, et al. Analysis of Aurora B kinase in non-Hodgkin lymphoma. *Lab Invest* 2009;89:1364–73.
  26. Pearson T, Shultz LD, Miller D, et al. Non-obese diabetic-recombination activating gene-1 (NOD-Rag1 null) interleukin (IL)-2 receptor common gamma chain (IL2r gamma null) null mice: a radioresistant model for human lymphohaematopoietic engraftment. *Clin Exp Immunol* 2008;154:270–84.
  27. Unwin RD, Pierce A, Watson RB, et al. Quantitative proteomic analysis using isobaric protein tags enables rapid comparison of changes in transcript and protein levels in transformed cells. *Mol Cell Proteomics* 2005;4:924–35.
  28. Ran D, Schubert M, Pietsch L, et al. Aldehyde dehydrogenase activity among primary leukemia cells is associated with stem cell features and correlates with adverse clinical outcomes. *Exp Hematol* 2009;37:1423–34.
  29. Gal H, Amariglio N, Trakhtenbrot L, et al. Gene expression profiles of AML derived stem cells; similarity to hematopoietic stem cells. *Leukemia* 2006;20:2147–54.
  30. Muranyi AL, Dedhar S, Hogge DE. Targeting integrin linked kinase and FMS-like tyrosine kinase-3 is cytotoxic to acute myeloid leukemia stem cells but spares normal progenitors. *Leuk Res* 2010;34:1358–65.
  31. Xie W, Wang X, Du W, et al. Detection of molecular targets on the surface of CD34+ CD38- bone marrow cells in myelodysplastic syndromes. *Cytometry A*. 2010;77:840–8.
  32. Lacraz S, Nicod LP, Chicheportiche R, et al. IL-10 inhibits metalloproteinase and stimulates TIMP-1 production in human mononuclear phagocytes. *J Clin Invest* 1995;96:2304–10.
  33. Stearns ME, Fudge K, Garcia F, et al. IL-10 inhibition of human prostate PC-3 ML cell metastases in SCID mice: IL-10 stimulation of TIMP-1 and inhibition of MMP-2/MMP-9 expression. *Invasion Metastasis* 1997;17:62–74.
  34. Heissig B, Hattori K, Dias S, et al. Recruitment of stem and progenitor cells from the bone marrow niche requires MMP-9 mediated release of kit-ligand. *Cell* 2002;109:625–37.
  35. Pal-Ghosh S, Blanco T, Tadvalkar G, et al. MMP9 cleavage of the  $\beta$ 4 integrin ectodomain leads to recurrent epithelial erosions in mice. *J Cell Sci* 2011;124:2666–75.
  36. Iwata S, Kobayashi H, Miyake-Nishijima R, et al. Distinctive signaling pathways through CD82 and  $\beta$ 1 integrins in human T cells. *Eur J Immunol* 2002;32:1328–37.
  37. Berditchevski F, Kraeft SK, Chen LB, et al. Transmembrane-4 superfamily proteins CD81 (TAPA-1), CD82, CD63, and CD53 specifically associated with integrin  $\alpha$ 4  $\beta$ 1 (CD49d/CD29). *J Immunol* 1996;157:2039–47.
  38. Matsunaga T, Takemoto N, Sato T, et al. Interaction between leukemic-cell VLA-4 and stromal fibronectin is a decisive factor for minimal residual disease of acute myelogenous leukemia. *Nat Med* 2003;9:1158–65.
  39. Papayannopoulou T, Priestley GV, Nakamoto B. Anti-VLA4/VCAM-1-induced mobilization requires cooperative signaling through the kit/mkit ligand pathway. *Blood* 1998;91:2231–9.
  40. Byk T, Kahn J, Kollet O, et al. Cycling G1 CD34+/CD38+ cells potentiate the motility and engraftment of quiescent G0 CD34+/CD38-/low severe combined immunodeficiency repopulating cells. *Stem Cells* 2005;23:561–74.
  41. Zheng Y, Sun A, Han ZC. Stem cell factor improves SCID-repopulating activity of human umbilical cord blood-derived hematopoietic stem/progenitor cells in xenotransplanted NOD/SCID mouse model. *Bone Marrow Transplant* 2005;35:137–42.
  42. Nervi B, Ramirez P, Rettig MP, et al. Chemosensitization of acute myeloid leukemia (AML) following mobilization by the CXCR4 antagonist AMD3100. *Blood* 2009;113:6206–14.
  43. Saito Y, Uchida N, Tanaka S, et al. Induction of cell cycle entry eliminates human leukemia stem cells in a mouse model of AML. *Nat Biotechnol* 2010;28:275–80.
  44. He B, Liu L, Cook GA, et al. Tetraspanin CD82 attenuates cellular morphogenesis through down-regulating integrin  $\alpha$ 6-mediated cell adhesion. *J Biol Chem* 2005;280:3346–54.
  45. Christensen JG, Burrows J, Salgia R. c-Met as a target for human cancer and characterization of inhibitors for therapeutic intervention. *Cancer Lett* 2005;225:1–26.
  46. Danilkovitch-Miagkova A, Zbar B. Dysregulation of Met receptor tyrosine kinase activity in invasive tumors. *J Clin Invest* 2002;109:863–7.
  47. Tesio M, Golan K, Corso S, et al. Enhanced c-Met activity promotes G-CSF-induced mobilization of hematopoietic progenitor cells via ROS signaling. *Blood* 2011;117:419–28.
  48. Marreiros A, Dudgeon K, Dao V, et al. KAI1 promoter activity is dependent on p53, junB and AP2: evidence for a possible mechanism underlying loss of KAI1 expression in cancer cells. *Oncogene* 2005;24:637–49.
  49. Jackson P, Ow K, Yardley G, et al. Expression and clinical significance of p53, JunB and KAI1/CD82 in human hepatocellular carcinoma. *Hepatobiliary Pancreat Dis Int* 2009;8:389–96.

journal homepage: [www.elsevier.com/locate/febsopenbio](http://www.elsevier.com/locate/febsopenbio)

## Calretinin mediates apoptosis in small cell lung cancer cells expressing tetraspanin CD9<sup>☆</sup>

Ping He<sup>a,c,1</sup>, Hanako Kuhara<sup>a,1</sup>, Isao Tachibana<sup>a,\*</sup>, Yingji Jin<sup>a</sup>, Yoshito Takeda<sup>a</sup>, Satoshi Tetsumoto<sup>a</sup>, Toshiyuki Minami<sup>a</sup>, Satoshi Kohmo<sup>a</sup>, Haruhiko Hirata<sup>a</sup>, Ryo Takahashi<sup>a</sup>, Koji Inoue<sup>a</sup>, Izumi Nagatomo<sup>a</sup>, Hiroshi Kida<sup>a</sup>, Takashi Kijima<sup>a</sup>, Tetsuji Naka<sup>a,d</sup>, Eiichi Morii<sup>b</sup>, Ichiro Kawase<sup>a</sup>, Atsushi Kumanogoh<sup>a,e</sup>

<sup>a</sup>Department of Respiratory Medicine, Allergy and Rheumatic Diseases, Osaka University Graduate School of Medicine, Osaka 565-0871, Japan

<sup>b</sup>Department of Pathology, Osaka University Graduate School of Medicine, Osaka 565-0871, Japan

<sup>c</sup>Department of Respiratory Medicine, The Second Affiliated Hospital, School of Medicine, Xi'an Jiaotong University, Xi'an 71004, China

<sup>d</sup>Laboratory of Immune Signal, National Institute of Biomedical Innovation, Osaka 567-0085, Japan

<sup>e</sup>CREST, JST, Department of Immunopathology, WPI Immunology Frontier Research Center, Osaka University, Osaka 565-0871, Japan

### ARTICLE INFO

#### Article history:

Received 17 January 2013

Received in revised form 5 April 2013

Accepted 26 April 2013

#### Keywords:

Small cell lung cancer

Proteomics

Tetraspanin

CD9

Calretinin

Apoptosis

### ABSTRACT

**A majority of small cell lung cancer (SCLC) cells lack a metastasis suppressor, tetraspanin CD9, and CD9 expression promotes their apoptosis. By a proteomics-based approach, we compared an SCLC cell line with its CD9 transfectant and found that a calcium-binding neuronal protein, calretinin, is upregulated in CD9-positive SCLC cells. Ectopic or anticancer drug-induced CD9 expression upregulated calretinin, whereas CD9 knockdown down-regulated calretinin in SCLC cells. When calretinin was knocked down, CD9-positive SCLC cells revealed increased Akt phosphorylation and decreased apoptosis. These results suggest that CD9 positively regulates the expression of calretinin that mediates proapoptotic effect in SCLC cells.**

© 2013 The Authors. Published by Elsevier B.V. on behalf of Federation of European Biochemical Societies. All rights reserved.

### 1. Introduction

Small cell lung cancer (SCLC) is highly malignant lung tumor that spreads early throughout the body. It is characterized by neuroendocrine features such as neuropeptide production and N-CAM expression [1]. At diagnosis in most cases, SCLC has already metastasized to regional lymph nodes and distant organs including brain, bone, liver, and adrenal gland, thus excluding the possibility of surgical resection. Currently, standard treatment against extended SCLC is chemotherapy including cisplatin and etoposide [2]. Despite its high sensitivity to these anticancer drugs, SCLC rapidly develops recurrent tumors locally and at the distant organs. Such malignant phenotype is at least partially caused by acquired resistance to apoptotic cell death [3]. Elucidation of its mechanisms is necessary to improve outcome

of chemotherapy, but little has been clarified.

Tetraspanins are a family of membranous proteins that has characteristic structure spanning the membrane four times. Through association with other functional proteins including integrins, growth factor receptors, membrane proteases, and intracellular signaling molecules, tetraspanins organize multiprotein complexes at the tetraspanin-enriched microdomain (TEM) and regulate cell adhesion, migration, and survival [4,5]. Among 33 members in humans, CD9 and CD82 are known as a metastasis suppressor of solid tumors. Clinical and pathological findings suggest that decreased expressions of these tetraspanins are associated with progression of cancers of breast, pancreas, colon, and esophagus, and nonsmall cell lung cancer (NSCLC) and thus with poor prognosis [6,7].

We have shown that, among tetraspanins, CD9 is selectively absent in a majority of SCLC lines and SCLC tissues in contrast to NSCLC which frequently expresses CD9, and that ectopic expression of CD9 in SCLC cells suppresses integrin  $\beta$ 1-dependent cell motility [8] and promotes apoptotic cell death through attenuation of PI3K/Akt signaling [9]. These results suggest that the absence of CD9 contributes to highly malignant phenotype of SCLC. We also found that CD9 expression is induced and cell motility is decreased when SCLC cells are exposed to cisplatin or etoposide [10]. In the present study, we compared an SCLC cell line with its CD9 transfectant by a proteomics-based approach and found that a calcium-binding neuronal protein,

<sup>☆</sup> This is an open-access article distributed under the terms of the Creative Commons Attribution License, which permits unrestricted use, distribution, and reproduction in any medium, provided the original author and source are credited.

Abbreviations: SCLC, small cell lung cancer; NSCLC, nonsmall cell lung cancer; PARP, poly(ADP-ribose)polymerase; PMF, peptide mass fingerprinting; MALDI-TOF, matrix-assisted laser desorption/ionization time-of-flight; RT-PCR, reverse transcription-PCR; KO, knockout

<sup>1</sup> These authors contributed equally to the study.

\* Corresponding author. Tel.: +81 6 6879 3833; fax: +81 6 6879 3839.

E-mail address: [itachi02@med3.med.osaka-u.ac.jp](mailto:itachi02@med3.med.osaka-u.ac.jp) (I. Tachibana).

calretinin, is upregulated in CD9-positive SCLC cells. We also show that calretinin mediates apoptotic cell death of SCLC.

## 2. Materials and methods

### 2.1. Cell lines

OS1, OS2-RA, and OS3-R5 were SCLC cell lines established in our laboratory, and their biological properties were previously characterized [8]. SCLC lines, OC10 and CADO LC6, a lung adenocarcinoma cell line, CADO LC9, and a mesothelioma cell line, OC-(MT)37, were provided by Osaka Medical Center for Cancer and Cardiovascular Diseases (Osaka, Japan) [11]. An SCLC line, SBC-3, and its chemoresistant subline, SBC-3/CDDP, were kindly provided by Dr. K. Kiura (Okayama University, Okayama, Japan) [10]. SCLC cell lines, NCI-H69, NCI-N231, and NCI-H209, a lung adenocarcinoma line, A549, and pleural mesothelioma lines, NCI-H226, NCI-H2452, NCI-H28, and MSTO-211H, were purchased from American Type Culture Collection (Rockville, MD). A lung squamous cell carcinoma line, HARA, was a kind gift from Dr. H. Iguchi (Kyusyu Cancer Center, Fukuoka, Japan). All cell lines were maintained in RPMI 1640 medium supplemented with 10% heat-inactivated FBS, 100 U/ml penicillin, and 100 µg/ml streptomycin.

### 2.2. Antibodies and reagents

Mouse anti-CD9 mAb (MM2/57), anti-poly(ADP-ribose)polymerase (PARP) mAb (42/PARP), and anti-β-actin mAb (C4) were purchased from Biosource, BD Biosciences, and Santa Cruz Biotechnology, respectively. Mouse anti-CD9 mAb (72F6) was purchased from Novocastra. Goat anti-calretinin polyclonal Ab (AB1550) and rabbit anti-calretinin polyclonal Ab (DC8) were purchased from Chemicon International and Zymed Laboratories, respectively. Rabbit anti-cleaved PARP (Asp214) mAb (D64E10), anti-phospho-Akt (Ser473) mAb (D9E), and anti-Akt polyclonal Ab were purchased from Cell Signaling Technology. Cisplatin (CDDP) was provided by Nippon Kayaku Co. (Tokyo, Japan).

### 2.3. Flow cytometry

Cells ( $10^4$ ) were incubated with 10 µg/ml primary mouse mAbs and labeled with FITC-conjugated goat anti-mouse immunoglobulin (Biosource International). Normal mouse IgG was used as a control. Stained cells were analyzed on a FACScan (Becton Dickinson).

### 2.4. cDNA and small interfering RNA (siRNA) transfection

Establishment of stable CD9-, NAG-2-, and mock-transfectants of OS3-R5 was previously described [8,9]. Cells were transfected with 40 nM cocktail siRNAs against human CD9 (No. SHF27A-0631; B-Bridge International) or human calretinin (No. SHF27A-0981; B-Bridge International), or negative control cocktail RNAs (No. S30C-0126; B-Bridge International) using LipofectAMINE 2000 Reagent (Invitrogen).

### 2.5. Two-dimensional electrophoresis (2-DE) and mass spectrometry analysis

Proteins were extracted from cells with the Complete Mammalian Proteome Extraction Kit (Calbiochem, Darmstadt, Germany). For 2-DE, isoelectric focusing (IEF) was performed using the PROTEAN IEF cell (Bio-Rad laboratories) according to the manufacturer's instructions. Extracted proteins were reconstituted in a rehydration buffer (7 M urea, 2 M thiourea, 4% CHAPS, 2 mM tributylphosphine (TBP), 0.0002% bromophenol blue (BPB), 0.2% Bio-lyte ampholyte 4–7) and applied to ReadyStrip™ IPG strips (11 cm, pH 4–7). IEF was run for 45,000 Vh. Two-dimensional electrophoresis was carried out in 10% Bis-Tris Criterion™ XT Precast gels. After staining with the Silver

Stain MS Kit (Wako Pure Chemical Industries, Osaka, Japan), the gels were captured by transmission scanning and analyzed with Image Master 5.0 (Amersham Biosciences). Following analysis, selected protein spots were manually excised from the gels and digested with trypsin (Promega) according to published procedures [12]. All peptide mass fingerprinting (PMF) spectra were obtained by using an ultraflex TOF/TOF matrix-assisted laser desorption/ionization time-of-flight (MALDI-TOF) mass spectrometer (Bruker Daltonics, Bremen, Germany).

### 2.6. Database search

PMF data were searched with Mascot software (Matrix Science, London, UK) against NCBI nr or Swiss-Prot databases. Protein database searching was performed with following parameters: *Homo sapiens*, maximum of one missed, cleavage by trypsin, monoisotopic mass value, charge state of 1+, allowing a mass tolerance of 100 ppm, and carbamidomethyl modification of cysteine. Protein scores of >64 indicate identity or extensive homology ( $P < 0.05$ ) and were considered significant.

### 2.7. Reverse transcription-PCR (RT-PCR)

One microgram of total RNA was reversely transcribed with a cDNA synthesis kit (Invitrogen) using random hexamers. The thermal cycling parameters were 30 cycles of 40 s at 94 °C, 40 s at 60 °C, and 90 s at 72 °C for CD9 and 30 cycles of 30 s at 94 °C, 30 s at 60 °C, and 90 s at 72 °C for calretinin. We confirmed that these variables yielded amplification of template DNAs within a linear range. The sequences of upstream and downstream oligonucleotide primers for CD9 was previously described [8]. Upstream and downstream oligonucleotide primers used for calretinin were 5'-GGAAGCACTTTGACGCAGACG-3' and 5'-CTCGCTGCAGAGACAATCTC-3', respectively.

### 2.8. Immunoprecipitation and immunoblotting

Cells were lysed in lysis buffer containing 1% Brij 99, 25 mM HEPES, pH 7.5, 150 mM NaCl, 5 mM MgCl<sub>2</sub>, 2 mM phenylmethylsulfonyl fluoride, 10 µg/ml aprotinin, and 10 µg/ml leupeptin. Whole cell lysates or immunoprecipitates with anti-CD9 mAb (MM2/57) were separated by 10% SDS-PAGE under nonreducing conditions for CD9 or under reducing conditions for the other proteins. After transfer to Immobilon-P membranes (Millipore), immunoblotting was performed with primary Abs followed by peroxidase-conjugated secondary Abs. Immunoreactive bands were visualized with a chemiluminescent reagent (PerkinElmer).

### 2.9. Immunohistochemistry

A human SCLC tissue array was purchased from US Biomax Inc. It contained small cell carcinoma tissues from 30 individuals and normal tissues from three individuals. Each specimen was represented by two cores from different tissue spots. After antigen retrieval, inactivation of endogenous peroxidase, and blockade of non-specific reaction, the tissue microarray sections were stained with anti-CD9 mAb (72F6) or anti-calretinin Ab (DC8), followed by incubation with biotinylated goat anti-mouse and rabbit IgG Ab and streptavidin-conjugated peroxidase. These were counterstained with Mayer's hematoxylin [10]. Specimens were regarded as positive when staining was observed in more than 30% of tumor cells on average. The significance of association between CD9 staining and calretinin staining was evaluated by Fisher's exact test.